UNIVERSITY OF LATVIA
FACULTY OF PHYSICS AND MATHEMATICS

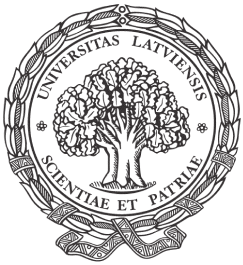

Sergejs Fomins

SHAPE AND COLOR IN IMAGE RECOGNITION

Summary of the Doctoral Thesis

Promotion to the Degree of Doctor of Physics
Subbranch: Medical Physics

Rīga, 2011

Thesis was developed in the period from 2006 to 2011
at the Faculty of Physics and Mathematics of the University of Latvia

Scientific advisor: *Dr. habil. phys.*, Prof. **Māris Ozoliņš**

Reviewers:

Dr. habil. phys., Prof. **Jānis Spīgulis**, Institute of Atomic Physics and Spectroscopy, University of Latvia

Dr. phys. **Jānis Teteris**, Institute of Solid State Physics, University of Latvia

Prof. **Henrikas Vaitkevicius**, Vilnius University

The defense of the PhD thesis will take place in an open session of the Promotion Council of Medicine Physics on 11th of February, 2011, at 15:00 in the conference hall of the Institute of Solid State Physics of University of Latvia.

Chairperson of the Specialized Promotion Council of the scientific section of Physics and Astronomy at the University of Latvia: *Dr. habil. phys.*, Prof. **Ivars Lācis**

The PhD Thesis and its summary are available
at the Library of the University of Latvia (4 Kalpaka Blvd, Rīga),
Latvian Academic Library (10 Rūpniecības Str.), and
at the Faculty of Physics and Mathematics of the University of Latvia (room F210).

© Sergejs Fomins, 2011
© University of Latvia, 2011

ISBN 978-9984-45-304-0

CONTENTS

ABSTRACT

Color and shape perception is processed in the ventral pathway of the primate visual system. Form perception in the hierarchical organization of the visual system starts in the primary visual cortex, there most of the simple cell neurons are tuned to the elongated oriented details of different spatial frequency, when in higher cortical areas details are organized into more complex structures. Parallel to the perception of forms color of the objects is perceived, when receptor signals are formed into the final perception. Thesis study simple form perception with textures, color perception and afterimages, as also the influence of form on the color perception. Experimental methods and results are advanced as practical applications for cases when color and form perception is imperfect.

Texture segregation characteristics are studied, depending on the orientation of contextual information around the stimuli, and improvements of responses after perceptual learning. Method provided by texture studied is used together with ferroelectric shutter goggles to improve the visual characteristics in the case of amblyopia.

To objectively analyze the performance of the pseudoisochromatic color vision diagnostic plates, solutions based on the multispectral imaging are offered. The methods of analysis uses chromatic sensitivities of human photopigments to model a performance of the defective color vision together with machine vision algorithms for the objective evaluation of the test diagnostic performance. The established method makes it possible to study pseudoisochromatic tables design and analyze applicability in different lighting conditions.

Despite the fact that cone sensitivities are well studied, color vision mechanisms of the visual cortex are a widely studied field these days. Color aftereffects are studied in the subjects with normal trichromatic color vision, as also in subjects with impaired color vision. The aftereffect identification method is proposed to be developed as an alternative method for diagnosis of color vision anomaly or deficiency.

Surface perception includes the processes of construction of shape based on the contour information with following assignment of the visible features, such as color, brightness and texture. Our between the contours filling-in study has shown that in the cortex form perception is related to the color processing. Colors that produce the strongest aftereffects in filling-in are not always complementary, and can give strong sensation between more than two colors. Identified strongest colors are not aligned along unique hue direction or cardinal directions of color space.

INTRODUCTION

Human visual system can be divided into two relatively distinct information processing streams: the dorsal pathway engaged in analysis of moving targets, and ventral pathway, responsible for form and color perception. This work is dedicated to the research of stimulus parameters - shape and color, processed in the ventral visual pathway, as also proposing practical application of the developed methods.

Perception of color starts in the retina where the light is perceived by the three types of cones and following signal transformation and conduction to the cortex. Due to genetic reasons a person could miss one, or some pigments, which results in functional individualities of color perception. The type and the degree of distortion depend on genetic factors, but all of them result in a certain inability to distinguish colors. There are various color vision testing techniques, and the most popular and easily applicable are pseudoisochromatic (PIC) plates, that help to determine the type of deficiency and degree of anomaly. However, not always these tests provide an unambiguous diagnosis. The reason for this may be the printed test page dilapidation or choice of improper lighting. To provide objective measures about usability of PIC plates, multispectral imaging of the plates was applied with the subsequent analysis. Spectral data along the whole spatial scale of the image can be converted into the cones sensitivity and algorithm applied to analyze PIC tests. The results are potentially important for analysis of existing PIC plates and the development of novel tests. Proposed method could help to save time by avoiding a need for clinical testing.

Shape perception begins with the analysis of simple oriented features. Visual scenes in the environment around us contain a myriad of such simple image details and processes in the primary visual cortex occur without the presence of attention. This makes the surface-oriented (or texture) for visual experiments on the visual cortex an excellent tool for preattentive process research. It is well-known that aging influences the learning process, when acquisition of new functions becomes more challenging. Perceptual learning is an important process, which guides us through our life, and especially specific to those people who lose functions and need to restore the capabilities to the normal conditions. The learning process shows the ability of the adult brain to retain its functions, which is the ability to learn and adapt to new circumstances and also visual stimuli, called plasticity. Texture stimuli are easy to apply for perceptual learning study, which would help to analyze the extent of the function improvement and repetitions needed to reach the saturated level.

Texture detection thresholds are dependent on several factors: the texture contrast, spatial frequency and color content. As a recent studies shows [1, 2],

the neural activity to stimuli is also dependent on the presence of stimuli besides the receptive field. Whether the periphery of an object orientation coincides with the central visual stimuli orientation makes a difference in response to the central stimuli. Previous studies that revealed the facilitative or suppressive influence of collinear stimuli on perception of central stimuli and the role of stimuli contrast in contextual modulation. At high contrast suppression of the response to the central stimuli is observed for iso-oriented stimuli, while for stimuli of low contrast the presence of high-contrast collinear periphery have facilitative influence [3]. Although contrast ratio is an important quality of the stimulus, it was shown that contextual modulation is a process affected by the time of stimuli presentation [4]. In our study we propose to examine the effect of iso- and ortho- oriented contextual effects on the large complex textured surface perception (in contradiction to simple Gabor patch) using temporally modulated stimuli of high contrast.

Most of the visual signals from the eye retina reach the cortex V1, which is the largest area of the visual system. Due to different reasons (refraction difference or optical occlusion) one of the eyes can be engaged much less in the vision process, which leads to insufficient development of the network of neural ways and results in impaired visual function in one of the eyes. Such a condition, when vision acuity is decreased without any physiological or anatomical impairment, is known as amblyopia ("lazy" eye) and subtends about 1-3% of the child population [5].The most used and effective method for amblyopia treatment is an occlusion therapy (or wearing of a patch) used on the better seeing eye, to promote the activity of the worse seeing eye to increase involvement in the visual process. In 2005, the Israeli company *Ophthocare* presented occlusion therapy using liquid crystal glasses, allowing the possibility to practice the weaker eye in sessions of different duration throughout the day. Method used for texture segregation together with liquid crystal goggles could be provided to attain the interaction of amblyopic and better seeing eyes. We propose to use a short duration temporal stimuli, similar to that for segmentation research, and subthreshold input from the better-seeing eye to improve the visual characteristics in the amblyopic eye.

The chromatic property`s of cortical neurons is a widely studied issue and there is still little known about the cortical processing of color in hierarchical levels of visual systems (V1, V2, V4 areas). Various phenomena and illusions are often observed in visual perception processes. Complex properties of the neural architecture of visual system lead to phenomena known as optical illusions. Well known are color after-images, which arise due to retinal pigment bleaching [6] and neural factors [7], also reported in recent binocular studies [8]. Prolonged observation of colored surfaces produces the sensation of after-image, which

results in a complementary color to the one physically present, and are identified by comparison techniques [9]. Nowadays stimuli can be carefully selected and displayed on a trichromatic calibrated monitor, as well as more accurate experimental methods for collecting participants responses are available, which can provide more precise data and possibility to analyze the data, based on physiological finding about the color vision mechanisms. There are a number of color vision deficiency simulations [10, 11], which allows converting color images to the simulations corresponding to each type of color vision deficiency. In simple words approach reflects hypothetical perception by protanopes and deuteranopes, when blue and yellow colors are separated and red appear similar to green colors. However, the precise color sensation is difficult to judge about. We offer to study the complementary hues of after-images in persons with color vision anomalies, which can have both theoretical and practical benefits. The individualities of after-image perception by anomalous color vision may be useful also for color vision testing.

The above mentioned after-images are closely related to the filling-in process, which is a preattentive mechanism of completion of missing information [12]. Comparing to the after-images, no prolonged exposition to stimuli is necessary to produce the filling-in effect, which supports the ideas of it as a neural process [9, 12]. Two chromatic shapes, followed by their contours, could be provided to study the chromatic properties of filling-in. If two of such differently colored stimuli are overlapped, the following choice of stimuli contours determines complementary between the contours filled in color. Such experimental setups could provide information about the neural attributes of color filling-in. unfortunately, it is difficult to evaluate after-image experienced in filling-in by direct matching. To evaluate the cardinal colors in the filling-in process we suppose to use the after-effect evaluation technique for two simultaneously presented colored objects. Our experimental idea is as follows: if two overlapped stimuli used to produce after-image are complementary to each other then strong filling-in will take place, which will cease till the colors become more similar. Hypothetically, if the filling-in is based on the retinal color processing it is expected to see strongest effect for complementary colors similar to that of the after-image hue experiments. We are interested to see if the complementaries of filing-in are related to the cardinal directions of color space and/or to unique hues.

GOALS AND TASKS

Thesis focuses on two major characteristics of the visual system – color and form, as also related impairments.

The goal of the work is to study perception of color and form at different levels of processing and find the practical applications of the developed results.

Tasks

1. To create stimuli and method for study of texture temporal perception dynamics and perceptual assessment of changes in the performance of perceptual training. Determine the influence of peripheral stimulation on recognition parameters of central stimulus.
2. Perform a multispectral acquisition of pseudoisochromatic plates for color vision testing. Find an algorithms and methodology to provide the quantitative measures of test performance under different lighting conditions.
3. To create a calibrated chromatic stimulus and to find a method of computerized identification of complementary hues of color after-images. Explore complementary hues of after-images for persons with normal color vision and for those with color vision impairments.
4. Provide a stimulus and method for evaluation of the influence of object shape on perception of color of the object.

THEORETICAL BACKGROUND

1.1. Hierarchical organization for form and color

Detailed understanding of cortical organization comes from anatomical and physiological studies of the areas of the brain [13]. Two main principles are distilled from the studies of visual areas.

The first principle states, that visual cortical areas are organized into processing streams, both of which originate from the primary visual cortex (V1), and both of which consists of multiple areas beyond V1. Ventral stream (or 'what' stream) is directed into temporal lobe and is crucial for the visual recognition of the objects, whereas dorsal stream ('where') is directed to the parietal cortex and is responsible for spatial relationships among objects and visual guidance toward them [13]. Lesion studies to the inferior temporal cortex (ventral stream) cause severe deficits on a wide range of visual discrimination tasks (objects, color, pattern and shape) [14].

The second principle of cortical organization is that within each of the processing streams, visual areas form processing hierarchies. Progressing forward along the ventral pathway, there is a general trend toward selectivity for increasingly complex stimulus features or combinations of features [13]. Form and color are processed in the ventral visual pathway and related areas can be aligned in the following hierarchical ascending sequence: V1, V2, V4 and PIT, TE (interior IT) [14].

1.2. Texture segregation

Texture segregation is the effortless division of a visual stimulus into distinct segments based on spatial gradients in local feature properties. Psychophysical studies suggest that texture segregation can be performed preattentively, or without necessary engagement of the attention [15]. In exploring people`s performance in T and L covered surfaces *J. Beck* hypothesized that displays containing a large number of elements could be grouped on the basis of their shape similarity, as predicted by principles of Gestalt psychology. However, it was discovered that the factors governing texture segregation are not necessarily the same as those that determine the shape similarity of the same elements when they are perceived as individual figures. It was concluded that texture segregation resulted from detecting differences in the feature density of certain simple attributes, such as line orientation, overall brightness, color, size, and movement. [16]

It was pointed out that textures could be discriminated in either of two ways: through normal texture segregation (preattentively), effortlessly and simultaneously over a whole visual field or through involvement of focused attention (attentively). [16]

Texture segregation research started an era of the computational modelling of attention and provided the background for binding together results of the psychophysical, cortex physiology and modelling research. [17]

1.3. Visual masking

Perception of visual stimuli is dependent on different attributes and in time domain preceding and a subsequent stimulus plays a role in perception of the central target. Visual masking is the reduction or facilitation of visibility of stimuli by introduction of the mask before or after it. Extensive studied on masking showed that it is a useful tool for exploring the dynamics of processing in the visual system. There are several assumptions of visual masking, provided by B. Breitmeyer. First, a stimulus of an interval of about 10 to 300 ms is required to obtain a measurable effect on behavior or conscious awareness. Second, there is an active processing of information during stimulus interval. Third and fourth assumption states, that processing can take place at several specialized levels of processing; there the responses of mask and target can interact. [18]

There are several types of masking. Forward masking occurs when the mask precedes the onset of a target, and backward masking occurs when the mask is presented after the target. When the target and mask onsets are synchronous is called simultaneous masking [18].

Visual processing is a dynamic, temporally evolving phenomenon and pattern masking can be useful for investigating the temporal sequence and levels of cortical feed-forward and re-entrant information processing required for recognition of stimuli ranging from simple geometric forms to faces and complex scenes. The phenomenon of backward pattern masking, particularly the counter-intuitive finding, that the mask can severely impede the visibility of the target even though the target is presented first. Masking can be used to study the temporal dynamics of visual perception. [18]

Different elements of the visual stimuli could be used as a mask, depending on the task of the experiment. For example, luminance, color, texture or noise, and peripheral mask (paracontrast or metacontrast) could be used to mask the target. Nine key properties of metacontrast masking are being provided by *G.Francis* [19], many of which are attributable also to backward masking. To name few most important for our study, are target duration, mask duration and contour. The duration of target plays significant role in perception, when the

mask is kept constant. Strength of mask increases with the duration of masking. However, usually stimuli onset asynchrony (SOA) could be a major factor which influences the target perception [18, 19]. If target and mask are composed of the contours, the broken contour mask (noisy contour mask) is more effective. [19]

1.4. Color vision deficiencies

Congenital color deficiency is caused by inherited photopigment abnormalities. The retina may be lacking in functional cone receptors or there may be only one or two cone pigments instead of three. Defective red-green deficiency is inherited genetically in an X chromosome and occurs in 8 % of men and 0,4 % of women. Poor perception of green associated with deuteranope deficiency is more common comparing to the poor red perception in protanomaly. [21, 22]

There are different techniques and tests for diagnosis of color vision deficiency and anomaly: anomaloscopes, arrangement tests (Farnsworth D-15, D-100), and pseudoisochromatic plates. The last mentioned are most popular and easily applicable. Pseudoisochromatic (PIC) plates are examples of color camouflage. The object and background of the test design are colored spots or patches of randomly aligned size and luminance. These particular properties provide size and luminance noise, so only color information can be used by an individual to detect the latent object. The colors of the background and test spots are aligned along the dichromate confusion lines, with the slight variations of luminance and chromatic saturation. [22]

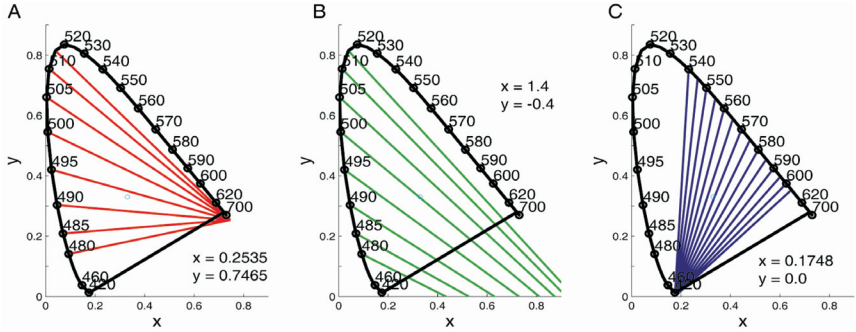

Fig. 1. **Dichromate confusion lines in CIE1931 x,y chromaticity diagram with convergence points for protanope (A), deuteranope (B) and tritanope (C) provided by Smith and Pokorny (1975) [23].**

Confusion lines (Fig. 1) represent the series of narrow zones in the CIE x,y chromaticity diagram with identically perceived colors for dichromatic vision.

Colors along the isochromatic lines look the same if no luminance difference is introduced between two colors. Isochromatic data for anomalous trichromats are similar to those of the corresponding dichromats, but do not include the complete range of chromaticities [22]. For this reason highly saturated colors can be perceived by anomalous vision, and small color changes should be used for classification of the severity of color anomaly. Dichromatic convergence points for isochromatic confusion lines are given for all three types of deficiencies [22, 23]. Figure 1depicts confusion lines and gives copunctal point for three deficiencies.

1.5. Color after-images

Steady prolonged viewing of a brightly colored stimulus can produce an experience of after-image. Chromatic after-effects are closely related to the phenomena of chromatic adaptation. Viewing a highly saturated color for a long time with fixed gaze causes perception of complementary hue in the corresponding retinal region in response to a neutral test field. [16]

Color after-images were traditionally thought to be of retinal origin although other psychophysical experiments indicate that their generation reflects also cortical processes [7, 8].

In the extensive study, after-image complementary hues were measured by means of the disk colorimetry method, long before the appearance of computers [24]. It was identified that the hue of the after-image is mainly determined by the hue of the stimulus color, and is independent of relative lightness and saturation. In the classic work by Wilson and Brocklebank it was found that additive complementary pairs used to produce the sensation of white are not the same as after-image pairs for blue-yellow and cyan-orange pairs. If one changes the saturation of the stimulus color the locus of after-image goes smoothly through the white point in the CIE x,y chromaticity diagram [24]. The great example of the color after-images could be provided by 'lilac chaser' illusion, proposed by Jeremy Hilton and popularized by Michael Bach. The illusion consists of the twelve magenta gaussian blobs with one of the blobs disappearing in clockwise direction, which produces the sensation of rotating green after-image after prolonged viewing of the stimuli. However, from the 1955 where was no extensive research on the complementary hues of after-images.

1.6. Filling-in

Filling-in is a remarkable perceptual phenomenon in which visual features, such as color, brightness, texture and motion, of the surrounding area are

perceived in a certain part of the visual field even though these features are not physically present [9].

As a visual function filling-in can be regarded as surface interpolation of missing information. Filling-in occurs in a variety of situations. Some of these situations have common characteristics, and can be divided into three main groups according to Komatsu [9]. Filling-in can arise in cases of deficits of visual inputs, like in a blind spot or scotoma. Surfaces can be filled-in when a steady fixation and stabilized retinal image is maintained. In the third case, neon color spreading and other illusions can produce this filling –in. [9, 20]

Alternately to after-images which result due to vanishing of pigment [7] filling-in is supposed to have a component of neural processing [7, 9, 12, 20].

Recently it was shown by Van Lier and colleagues (2009) how chromatic filling-in occurs between the contours of the shapes. In this study star shaped overlapping stimuli of two different colors were being used to produce the after-images. Subsequent presentation of contours of shapes produce after-images in color complementary to the chosen contours. [12]

It is commonly believed that such color filling-in phenomena are generated by neural circuitry that also process normal color perception, where early cortical areas are thought to fill-in colors by means of a contour-based filling-in mechanism [9].

2. TEXTURE SEGREGATION EXPERIMENTS

2.1. Perceptual learning with texture segregation

Fifteen persons participated in the texture segregation experiment, aged between 20 and 24 years (mean age 21.3 ± 1.4 years). Ten of the subjects performed an experiment with colored stimuli (five with red-green, and the other five with blue-yellow stimuli), and 5 with the black and white stimuli. Each of the participants performed the same experiment ten times. Segregation thresholds were calculated from the measured psychometric function in each of the 10 trials.

2.1.1. Stimuli and methods

An experimental stimulus is comprised of the Gabor gratings of different orientation. Gabor gratings are 5 by 5 mm large and are combined into hexagonal objects made up of 32 Gabor gratings. Two circular patches comprised of the Gabor gratings of the same orientation (diagonal or vertical) displayed on the horizontally oriented background are arranged on both sides of the fixation point. Angular dimension of one patch is 1.8 degrees from the 60 cm distance.

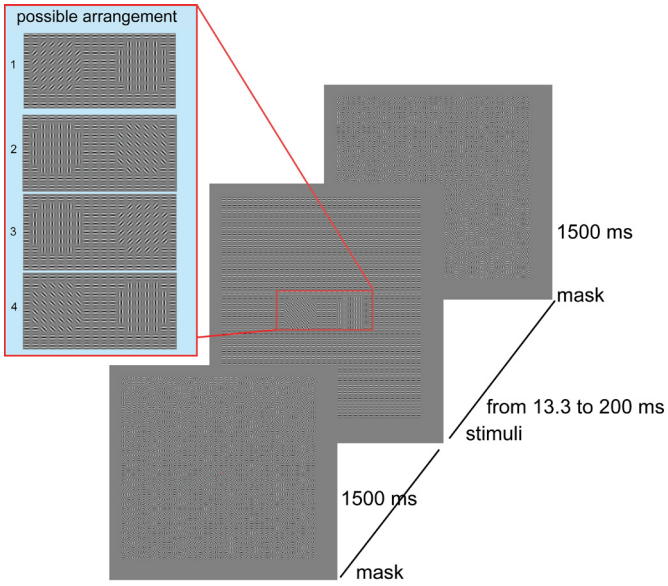

Fig. 2.1 **Experimental setup is produced by the mask presented for 1500 ms after which the stimuli is presented for times ranging from 13.3 to 200 ms. Stimuli could appear randomly in four different arrangement combinations.**

The stimuli are masked with a solid background of randomly oriented Gabor gratings. Each trial takes the exposition times from 13.3 till 200 ms

with a 1500 ms long mask in between the trials. The task for the subjects was to recognize the position (left or right) of the diagonally oriented Gabor patch (Fig. 2.1), in such a way providing a two alternative forced choice procedure.

Michelson contrast values were calculated for the three types of stimuli: high contrast black and white stimuli (94,6% ± 1,4%), red-green chromoluminous stimuli with luminance contrast 47,1% ± 0,3%, and blue-yellow stimuli with luminance contrast 67,4% ± 0,5%. All of the stimuli were presented on a 68,5 cd/m^2 luminous background.

Constant stimuli two alternative forced choice (2AFC) method was used for measurement of thresholds.

Experimental stimuli are presented on the 75 Hz refresh rate Samsung CRT monitor, controlled by CRS VISAGE stimuli generator.

2.1.2. Results

Measured psychometrical functions were fit by the Boltzmann sigmoid function (Eq.1) and 75 percent hit rates were defined as the recognition threshold. Fig. 2.2 shows the detection thresholds for three types of stimuli for all subjects.

$$y = \frac{A_1 - A_2}{1 + e^{(x - x_0)/dx}} + A_2, \qquad \text{(Eq. 1)}$$

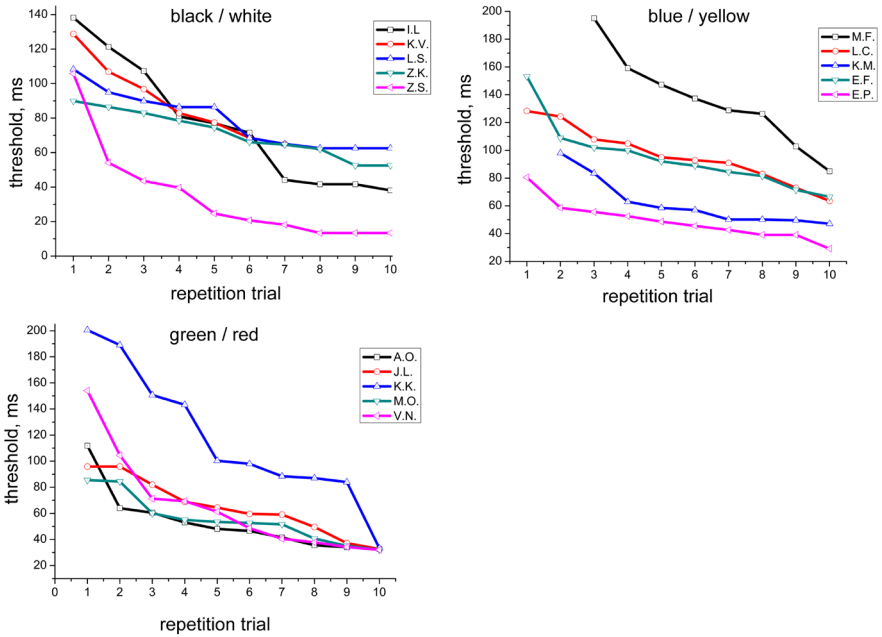

Fig. 2.2 **Thresholds for all subjects in each experiment repetition.**

When comparing the threshold times in these three groups of participants, it can be observed that the highest average decrease of the threshold is for the experiments with red-green stimuli, which are of the lowest contrast. The least change in the threshold values is observed in experiments with the black-white stimulus of high contrast. This could be explained by the difficulty of the task produced by the contrast of the stimuli, as the low contrast stimulus is more difficult to detect.

In our experiment we tried to detect the amount of repetitions necessary to achieve the lowest threshold level. The fastest results are obtained for the black-white stimuli; there almost linear curve response is gained at the 9th repetition trial. Large individual differences are present. For the blue-yellow stimuli lowest threshold is not obtained within the ten repetitions and individual differences are also present as in the case of black and white stimuli. For four of the subject response dynamics are the most close for red-green stimuli, which has the lowest contract value. In case of the red-green stimuli the lowest monotonous level is reached at the 9th repetition.

2.2. Contextual modulation in texture segmentation task

Three subjects with normal or corrected-to-normal vision took part in the experiment. All tasks were performed binocularly.

2.2.1. Materials and methods

All measurements were tested with the psychophysical two-alternative forced choice (2AFC) constant stimuli method in which the test target appeared at one of two locations, aligned to the right or to the left of the fixation point. Experimental stimuli were made as two oriented circular shaped objects; each consisted of 32 Gabor primitives. Each Gabor primitive consisted of 1.5 cycles and was presented in 0.46 degrees of visual angle.

Each circular object subtended 2.76 degrees of visual angle. The stimuli were presented as temporally modulated stimuli in seven different durations that varied from 13.3 to 93.3 ms on the background composed of the horizontally oriented Gabor primitives. The noisy orientation mask was produced from randomly oriented Gabor primitives of the same size and spatial frequency, and was applied for duration of a 3000 ms right after the test. Peripheral stimulation was produced by the square border 1.5 degrees wide. The border starts at the 3 degrees from the fixation point in the vertical direction and 5.5 degrees to the right and left from the fixation point.

The black-white temporally altered textures were shown on the horizontally oriented background where one of two objects contained Gabor primitives in

oblique directions but the other in a vertical direction. Subjects had to detect the object with oblique Gabor primitives as soon as possible. Collinear peripheral stimuli were added in the first part of the experiment and orthogonal in the second part of the experiment.

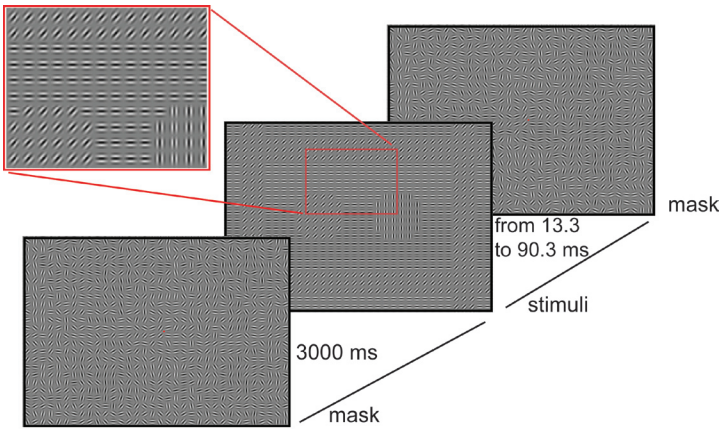

Fig. 2.3. **Stimuli and mask sequence. Stimuli expositions change from 13.3 to 90.3 ms with the 3000ms mask in between each of the trials.**

All items were presented on a grey background with a luminance of 67.6 cd/m^2. Michelson contrast for the black-white Gabor primitives was 94%. Luminance was determined with KONICA MINOLTA CS-100A chroma meter.

Each subject completed 60 measurements in 4 trials (15 measurements for one duration stimuli in 1 trial) for each of the seven test durations. Target orientation, duration order and target location were randomized.

Visual stimuli were presented with the CRS Visage stimulus generator on a CRT monitor at a 75 Hz refresh rate.

2.2.2. Results

Fig. 2.4 shows the results for all three subjects. All data are filled with the sigmoidal functions. In case of collinear peripheral stimuli answers are usually decreased 66.5 ms for two of participants (RP, SF). For subject LZ only statistical difference is identified for 39.99 ms duration stimuli between collinear and orthogonal condition. In case of the orthogonal contextual modulation psychometrical function is similar or shows at an even faster transition comparing to the no modulation conditions. The threshold for 2AFC procedure is 75 % of correct answers are obtained from the fitted Boltzmann sigmoidal functions. Threshold values are different for all three subjects; however changes

in the threshold expressed in percents for collinear modulation and no modulation conditions for all three subjects are 26% with standard error 4%. Thresholds identified for orthogonal stimulation show only slight change from the no modulation condition for subject RP and are similar to that of the no modulation condition for other two subjects.

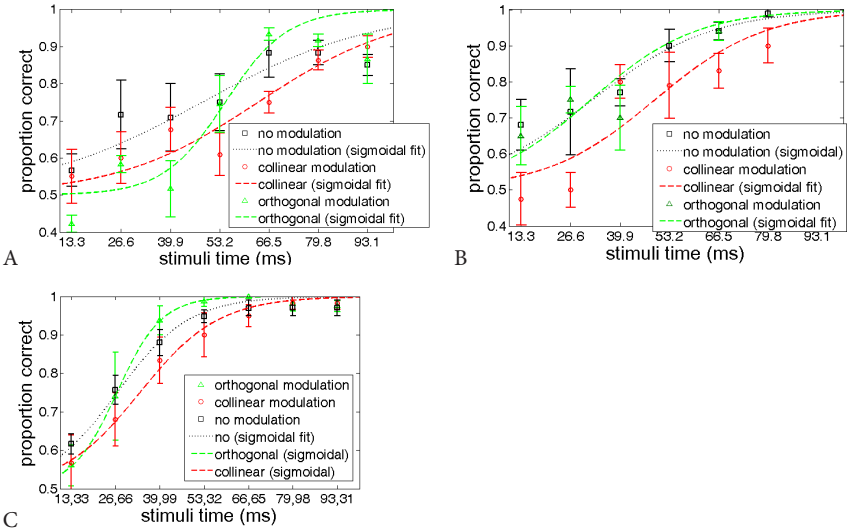

Fig. 2.4. **Psychometric functions of three experiment participants (A: RP, B: SF, and C: LZ).**

Primary visual cortex V1 is an anatomical structure that is strongly associated to simple texture segmentation tasks [3]. One of the popular explanations for contextual modulation is the existence of specific anatomical connections in V1. Horizontal connections within V1 spread over much larger distances than the size of receptive fields would necessitate [3].

There are previous texture segmentation studies where achromatic stimuli with different peripheral stimulation have been used [1, 2, 4, and 25]. In our study we have used larger stimuli (2.76°) with context starting at 3 degrees from the center of the test stimulus, to demonstrate contribution of iso- or ortho-oriented context on texture segmentation.

The rate of correct answers is decreased (suppression) mostly at middle stimuli duration times in texture segmentation task for temporally modulated stimuli. Contextual modulation in texture segmentation is strongly associated to the collinear peripheral stimulation. No effect, suppression or facilitation occurs in the case of orthogonal peripheral stimulation, but only suppression effects are observed in context of the collinear peripheral stimulation.

2.3. Application for amblyopia research

2.3.1. Introduction

Amblyopia is defined as the condition of low or reduced visual acuity not correctable by refractive means and not attributable to ophthalmoscopically apparent structural or pathologic anomalies or proven afferent pathway disorders. The oldest and the most popular therapy for amblyopia is a direct, opaque, total occlusion (e.g. patching of the good eye with a bandage). Such direct occlusion forces the patient to use the amblyopic eye to achieve the proper visual stimulation [26].

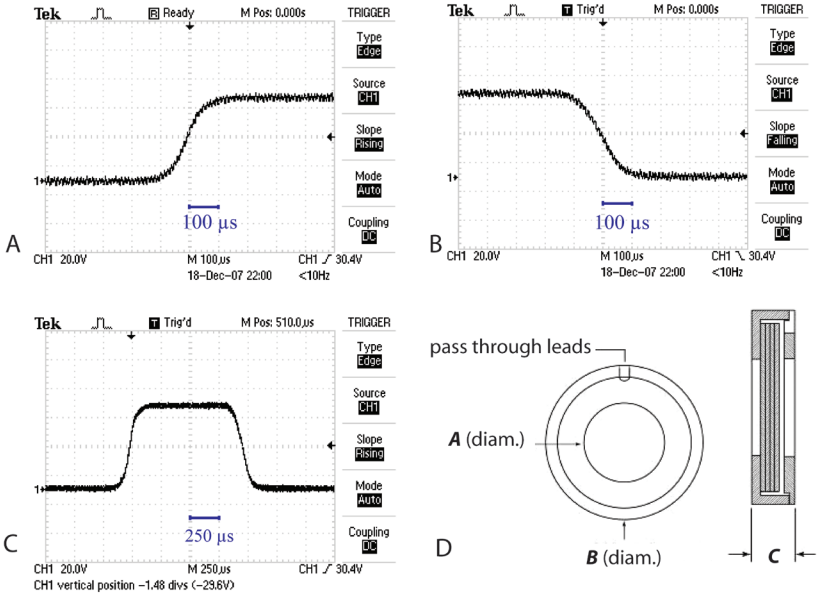

Fig. 2.5. **FLC glasses optical switching properties: attack rise time 200 µs (left); fall time 220 µs (centre); one impulse length – 1.25 ms (right graph). Data measured with Tektronix TDS2024B oscilloscope. Time scale on the X axis (100 µs per grid for 3A and 3B) and amplified voltage from the photodiode cell on the Y axis. The lowest voltage corresponding to closed shutter and peak voltage corresponding for the opened shutter. D: Shutter housing and physical dimensions: A-25.40 mm (aperture); B -37.85mm (diameter); C-6.90mm (thickness) (data from Displaytech data sheets [29]).**

Modern alternative of occlusion therapy was provided by *Ophthocare* (*www.opthocare.com*) presenting the liquid crystal goggles (LCG) as alternative to the opaque. The goggles comprise of a pair of electronic shutters, incorporated into

the optical refractive lens and worn in a spectacle manner. It is controlled by a preprogrammed microchip and is activated over the eye in short intervals. The 'close-open' sessions exercise the worse-seeing eye and enforce its use. Exercising of the amblyopic eye is performed all day long while glasses are worn. The goggles provide different session timings with shortest intervals starting from 5 seconds [27].

We propose to use ferroelectric liquid filters together with before mentioned method of dynamic brief visual stimulation, to maintain the training of the amblyopic eye and provide both eye interaction. Binocular interaction studies indicate a slight improvement in visual acuity in the amblyopic eye after perceptual training [28].

To produce the goggles for amblyopia research we use Displaytech (*www.displaytech.com*) shutters with flat transmission properties in the visible spectrum and also appropriate design that makes them easily mounted into the spectacle frame (Fig. 2.5). The FLC shutter offers exposure times of 0.0002 of a second while standard liquid crystal shutters may offer exposure times of only 0.01 of a second. These devices achieve a modulation depth of 30 db (or 1000:1 contrast ratio) [29]. Two such Displaytech shutters were incorporated into the spectacle frame to make it possible to use them on the eyes.

2.3.2. Stimuli and method

Our approach for amblyopia research with FLC comes from our previous experience based on the psychophysical studies with temporal brief stimuli [*Conferences Ref.4*]. Stimuli are presented in fast expositions ranging from 0.015 s to 0.150 s in 2AFC psychophysical design, while manual reaction times and proportion of correct answers are obtained. As the stimuli exposition time grows the decrease in manual reaction times can be observed. Such a paradigm should have a dramatic effect on reaction times for the worse-seeing eye, as the information processing in the cortical visual area V1 of the amblyopic eye path is impaired [30]. How much can the good eye help the bad eye to improve the processing and recognition rate, when the better-seeing eye input is activated for duration of milliseconds? This is the main question we address in our research.

Presented stimuli consisted of Snellen C letter optotypes oriented in different directions. The size of stimuli subtended 1.5 degrees on the screen for the viewing distance of 50 cm. Two stimuli were presented simultaneously to observer with the task to identify the optotypes with a diagonally oriented gap. The hundred trials were run in each of the series with ten responses per one exposition time.

The trials were performed for the good eye first, to know the best performance possible for a patient. After that a series of measurements of

reaction time for the worse eye were performed with the LCG on the eyes. The shutter on the worse-seeing eye was opened through the whole time of each trial and shutter on the better-seeing eye was opened for a moment with the latency of 12 ms after the beginning of the trial (Fig. 2.6). We have chosen 10, 7, 5, 2.5 and 1.25 ms long durations as the subthreshold stimulation for better-seeing eye according to experience of subject. Impulses over 10 ms were reported as obstructive, when the better-seeing eye starts to dominate.

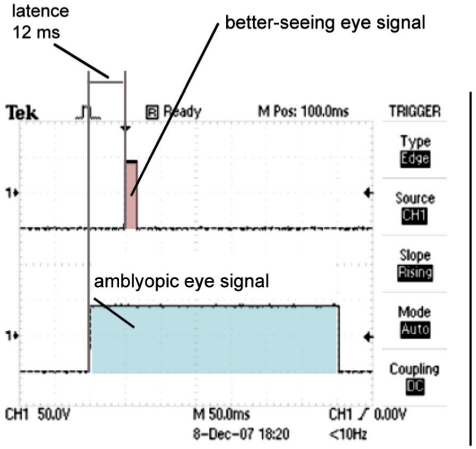

Fig. 2.6. **Impulse sequence rule of FLC glasses for right eye (top) and amblyopic left eye (bottom). Measurement of light transmitted through the left and right shutters. Measured by Tektronix TDS2024B oscilloscope.**

An amblyopic subject (33 years old) with the left amblyopic eye was engaged in the experiment. The decimal visual acuity for the right eye was 1.0 (60/60) point and for the amblyopic eye it was 0.35(9/60). Anisometropy was mentioned as the cause of amblyopia.

2.3.2. Results

In our experiment we have measured two quantities of the person's response: manual reaction time and psychometrical function for time varying stimuli. Psychometric functions for better-seeing eye signals are shown in Fig. 2.7.A. The black dashed line describes the response by the subject in carrying out experiments only with the left (worse) eye and the full black curve shows the response performing the task using the better-seeing eye. The best performance is seen at 7.5 ms and 5 ms auxiliary pulses. Threshold decrease produced by shorter (1.25, 2.5 ms) and longer pulses (10 ms) do not reach a performance as

good as obtained with the better-seeing eye. Detection threshold expressed in time units for the left eye is about 50 ms. Results for the right eye and also using subthreshold pulses of 5 and 7 ms indicate detection threshold at its maximum value of 16 ms.

Fig. 2.7.B shows the average reaction times for the better seeing eye (black line), amblyopic eye (red line) and supporting the amblyopic eye with pulse of 7.5 ms (green line). Carrying out the task with the right eye average reaction time is 580 ms while the slope for the amblyopic eye varies from 750 ms at the fast stimulus duration to 670 ms at the longer durations. Decreases of reaction time with auxiliary pulses have shown of about 100 ms improvements.

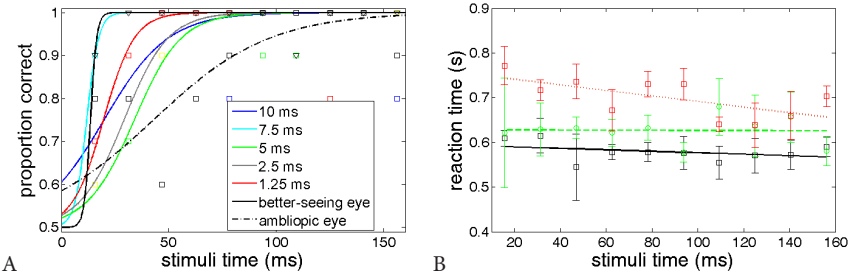

Fig. 2.7. **(A) Psychometric function for perception of brief stimuli with amblyopic eye and better-seeing eye with subthreshold stimulation. (B) Means reaction times of three measurements obtained running experiment with left eye (red), right eye (black) and with both eyes and auxiliary signal of 5 ms (green).**

2.3.3. Discussion

Records from monkey V1 cortex complex cells showed a strong reduction of responses to temporal stimulus in case of anisometropic amblyopia [31]. Latest visual evoked potential studies revealed that in anisometropic amblyopia evoked potential magnitude decreases more than twice. The signal delay (or latency) between amblyopic and normal eye reaches to 25 ms [32]. Fast goggles, which help control eye signals reaching each of the eyes, can be used to provide auxiliary signals through the better-seeing eye and improve perceptual characteristics of the amblyopic eye.

2.4. Conclusions

1. Texture segregation thresholds were defined in a perceptual learning paradigm using luminance and chromo-luminance Gabor patch stimuli (angular size 1.8 degrees, a contrast value: 95% (black-white), 47%

(red-green) and 67% (blue / yellow)), varying in time from 13 ms to 200 ms. Around a twice solid decrease in segregation threshold is observed as a result of trial repetition with the best improvement for chromatic stimuli of lowest contrast.

2. Contextual modulation effect was studied for experienced subjects with large Gabor patch stimuli (2.76°) and peripheral stimulation starting at 5.5x3° from the fixation point. First, it was found, that the orthogonal context not significantly alters the dynamics of perception. Secondly, collinear contextual stimulation produces suppressive effect and increased segregation threshold by 26%.
3. Experiments for the amblyopic subject with temporal stimuli showed a perception threshold in worse-seeing eye of 30 ms slower that in the good-seeing eye. Stimulation of the better-seeing eye with subthreshold temporal signal (from 1.25 to 10 ms) significantly improves detection in the amblyopic eye. The best results, similar to that of the better-seeing eye performance, are obtained at 5 ms stimulation.

3. MULTISPECTRAL COLOR ANALYSIS FOR EVALUATION OF PSEUDOISOCHROMATIC COLOR DEFICIENCY TESTS

3.1. Introduction

The extended version of the analysis of color deficiency tests could be provided by novel multispectral imaging techniques that allow acquisition of the spectrum of the test over the whole spatial extent. This allows for the possibility to apply two-dimentional image processing techniques over the test surface at any spectral channel of the visible spectrum. This allows more thorough analysis of the spatial patterns carried by the test color information.

The main goals of our research is to find a methodology that could be applied for the analysis and characterization of pseudoisochromatic plates using multispectral data and to find the ways to characterize the test performance without the presence of a subject.

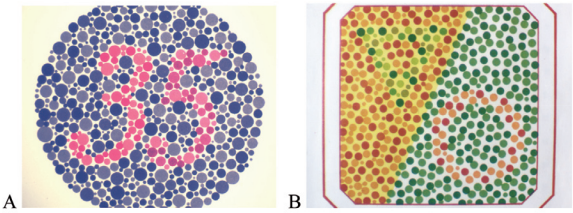

Fig. 3.1. **Ishihara test plate No13 (left). Rabkin test plate No17 (right). RGB representations of the tests are given.**

Ishihara`s test for color blindness test (Concise ed.) was available for our analysis. Ishihara`s test plate No 13, which discerns between the protanope, deuteranope deficiencies and helps to identify the severity of anomaly [33, 34], was chosen for analysis. The diagnostic plate is designed to be seen by normal subjects with color vision defectives seeing one number more easily than another. Normal subjects see numbers '3' and '5', protanopic gene carrier would perceive only '3' and deuteranope sees '5'. The second test available at the Optometry and Vision Science Department is a Rabkin's polychromatic tables, which incorporate the same design and plate with the similar diagnostic value as can be found in the Ishihara`s No13. Plate No 17 from Rabkin's test was chosen for analysis. This plate also contains hidden objects: a circle that cannot be seen by protanope and protanomalous persons and a triangle is unseen by deuteranope

and deuteranomalous. Ishihara`s plate detects two levels of anomaly and Rabkin is to detect three severity levels of anomaly. From this it can be supposed, that hidden objects spots in case of Ishihara test contain two hues and Rabkin test there are spots of three colors.

3.2. Experimental

For the acquisition of the spectral images we used the CRI Nuance Vis 07 spectral imaging system for microscopy. A Nikon AF Micro-Nikkor 60 mm f2.8D objective was mounted on the camera instead of the microscope. Correction was applied to avoid the geometrical decrease of the illumination in the periphery produced by the objective. To be sure about the spectral characteristics of our multispectral equipment CERAM white standard sample was measured with Ocean Optics USB400VIS through the calibrated optic fiber spectrometer and compared to the same measurement of the sample with the multispectral camera. A correction coefficient was applied to maintain the precise spectral measurements with the CRI Nuance camera.

Measurements were taken in the grey room adequately lit by daylight on a sunny day. The reflection spectra from the CERAM white standard measured with the spectrometer is shown in the Fig. 3.2 for the daylight and fluorescent illumination. Both spectra measured with exposition time of 1s. The white sample was measured also with a Konica Minolta CS100A chroma meter to check for the consistency of the calculated colorimetric values.

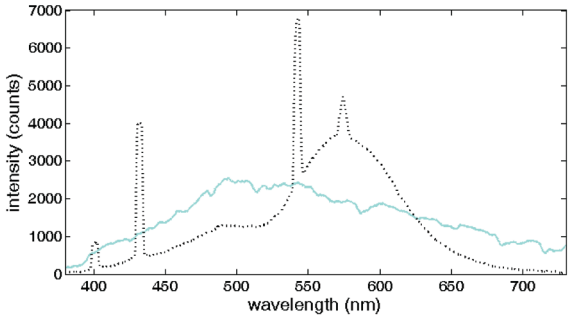

Fig. 3.2. **Reflectance spectrum obtained from the CERAM white standard sample under daylight (solid curve) and fluorescent illumination (dashed curve).**

In our analysis we have used spectral sensitivities' of human cones provided by Stockman et al [35].

According to the fact that protanope carriers are missing L cones and deuteranope carriers are missing M cones [22], we propose to use the following

expression to produce the representation of the anomalous ($0 < a, b < 1$) and deficient color vision (a or $b = 0$, only one signal is provided):

$$DS = a^*L - b^*M \tag{2}$$

However we were not sure about input from the S cones, and in our analysis we tried to check for the two cases, without the S cone signals Eq.2 takes a^*L – b^*M and with S cones input [36] (see Fig. 3.3):

$$DS = a^*L - b^*M - S. \tag{3}$$

For example, then M signal is missing perception reduces to L-S. The decrease of coefficient a shows the disappearances of the latent object corresponding to protanope deficiencies and changes to b influence the appearance of the latent object in deutran deficiency cases.

Whet the S signal is not taken into the account, L – M corresponds to the 'sensation' of the normal color vision subject (Fig. 3.3). However, the use of the Eq. 2 leads to the situation when the latent figures are almost unseen with a or b. At this point of analysis the S signal input influence is obvious for Ishihara`s PIC plate.

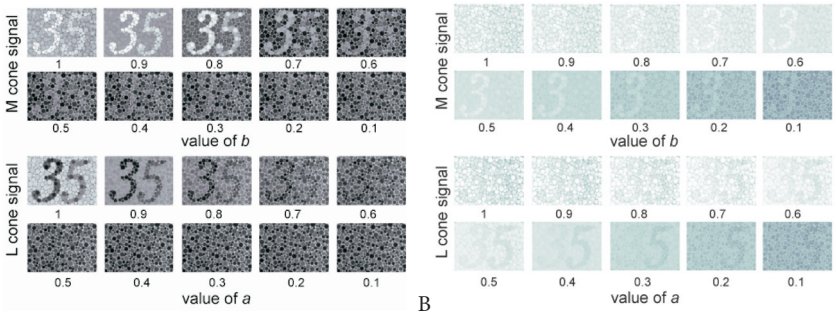

Fig. 3.3. **(A) Resulting simulation for dichromatic vision for Ishihara plate No13. First two rows show the decrease of M signal (deuteranopic) and row 3 and 4 show decrease of L signal (protanopic). (B) Results of the simulation including the S cone constant signal input.**

Simulated images in Fig. 5.3 are normalized to be represented on 8 nit systems. However, to objectively define the presence of the latent test object we propose a two dimensional cross-correlation procedure, technique used in machine vision applications of pattern matching. The latent test object can be

cross-correlated with that of the high contrast identical black white object. For this purpose the latent objects were extracted from the plate image and provided in maximum contrast (Fig. 3.4 C).

The background of the test was extended (Fig. 3.4 B), so at least half of the test object could be placed to all four directions. The equation 4 below is cross-correlation procedure taken between the high contrast latent test object and the extended version of the test.

$$X(i,j) = \sum_{m=0}^{Ma-1} \sum_{n=0}^{Na-1} TBE(m,n) \otimes (O(m+i, n+j)), \tag{4}$$

for $0 < i < M_a + M_b - 1$ and $0 < j < N_a + N_b - 1$.

The M_a and N_a in Eq. 4 are the dimensions of matrix TBE (test with extended background); M_b and N_b are the dimensions of matrix ***O*** (object of high contrast).

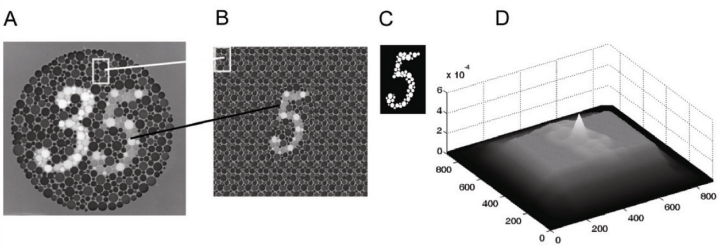

Fig. 3.4. **(A) Simulation for plate No 13 with L=1, M=0.7 signal proportion. (B) Extracted latent test object ('five') and extended background for better cross-correlation procedure. (C) High contrast test object to apply cross-correlation with. (D) Result of cross-correlation of B and C.**

The peak of the correlation value together with the ground noise level can be used to calculate the contrast, which can be interpreted as a measure of visibility of the latent test object. Weber contrast is commonly used when the average luminance is approximately equal to the background luminance and it is calculated as

$$C_w = \frac{I - I_b}{I_b}, \tag{Eq. 5}$$

where ***I*** is a luminance (peak in our case) and $\boldsymbol{I_b}$ is a background (ground noise value).

3.3. Results

Weber contrast values were calculated for different proportions of *a* and *b* (Fig. 3.4). In conditions when the S cone signal is not included in the calculation the Weber contrast value usually decreases together with the cones signal decrease. The two upper graphs in the Fig. 3.5 show results for Ishihara plate No 13 under daylight illumination (left graph) and halophosphate phosphor fluorescent lamps (right graph). In both cases the latent objects for deutran carriers are of lower contrast and approximately coincide with the protanope latent object contrast after decrease of signals.

The bottom graphs of Fig. 3.5 shows contrast values with S cone signal subtracted from the *a*L-*b*M. It can be clearly seen that latent objects of the best contrast corresponds to the idea of the test. Object '3' is seen by the protanope carriers and is of higher contrast and object '5' is for the deuteranopic carriers. Contrast values for both mentioned cases are very close, except values of *a* and *b* less than 0.5.

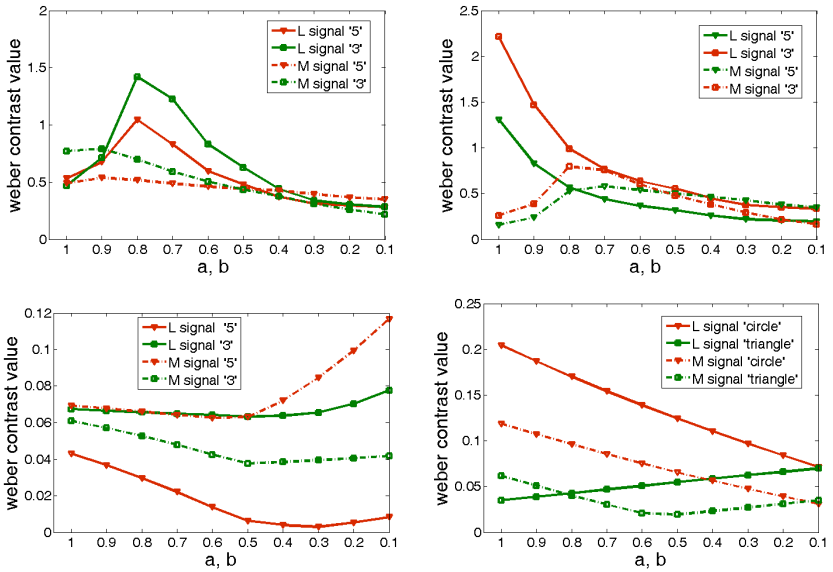

Fig. 3.5. **Weber contrast values of the cross-correlation results. Top left: shows values calculated for the daylight illuminated plate; top right shows Weber contrast values obtained for same plate No13 under fluorescent illumination. Bottom left: Ishihara plate No 13 with S cone signal present. Bottom right: Rabkin plate No 17 with S cone signal present.**

When the L and M proportion is set to that of the normal subject, contrast values for the protanope images usually are higher. The same can be said if the illumination change happens. However, illumination changes produce shifts in the colorimetric values of the chromatic content.

For the Rabkin test plate No 17 results are depicted in the right bottom graph of Fig. 3.5. This test follows similar logic. Protanope carriers would see a triangle object and deutran carriers are suggested to see a circle. When the L cone signal is decreased the circle object has dominant contrast values. Decrease of M cone ratio also results in more pronounced contrast for the circle stimuli.

The result of our analysis shows that Ishihara test plate No 13 has a better performance than the Rabkin test plate No 17 under the lit daylight illumination.

3.4. Discussion

Obtained results indicate that the Ishihara test is appropriate for color vision testing under daylight illumination in context of the used analysis. Many of the research support high clinical performance and colorimetric precision of the Ishihara pseudoisochromatic plates [37, 38, 39].The new approach of multispectral analysis gives us some insights into the details previously ignored or difficult to study. Spectral data of each pixel of image gives an opportunity to manipulate the data spatially in two dimensions. This makes two dimensional procedures as cross-correlation and object recognition possible, which can be valuable tools for the creation of new color deficiency tests. Cross-correlation procedure, or related techniques, could help to characterize the performance of the test without the presence of the observer. Availability of spatial data allows studying the tests in the modern context of the color appearance models, which include different attributes of human visual system, as adaptation, color contrast and color induction [40, 41]. Such an analysis is a digital alternative to the clinical evaluation of pseudoisochromatic tests and can be implemented taking into account different illumination conditions. Our approach in some way is similar to the techniques of simulation of dichromacy [10, 11]. Even we have used the word simulation; the idea of our study is to find the tools for characterization of the performance and clinical validity of tests, and not to characterize the perception by dichromate observer.

3.5. Conclusions

1. Multispectral images of color deficiency tests are acquired in the visible light spectral range from 420 to 720 nm, with a pitch of 10 nm in spatial angle of 7.7x9.5 degrees with a spatial pixel size of 0.1 mm.
2. Simulating deuteranope and protanope missing cone signals and using cross-correlation technique, we propose analytical method for pseudoisochromatic plate's performance analysis. Results of simulation show the better performance of Ishihara (No 13) over Rabkina test (No 17) in the daylight conditions.
3. The impact of the lighting can be taken into consideration for our method. We suggest using the proposed techniques for exploration of existing plates and development of the novel pseudoisochromatic plates.

4. COMPLEMENTARY HUES OF AFTER-IMAGES

4.1.1. Subjects, stimuli and method

Two male and three female subjects participated in the experiment. Participants' mean age was 24.2 ± 2.3 years. All participants of the experiment had no color vision deficiencies and corrected eye sight.

Color after-image evaluation method was set up with stimuli based on visual illusions "Lilac Chaser" principle [42]. Stimuli consist of 12 circular patches, arranged in a circular format, creating a clock like combination (Fig. 4.1). Background of the stimuli is chosen gray (RGB=128, 128, 128) with CIE coordinates x=0.35, y=0.39 with luminance 25 cd/m^2. During the experiment, 11 of the 12 circles are present and one of the patches disappears in clockwise directions for 400 ms. Following prolonged viewing of the stimuli, the sensation of the rotating patch of complementary color is produced. In the center of the experimental stimuli the adjustment patch is placed. There are two fixation squares given besides the point of central symmetry. The rationale for using two fixation points comes from our experience change of perception of color of central area after prolonged matching. The gaze is switched between two fixation squares, which help to move the matching patch, as also stimuli to the different retinal location. The angular size of the chromatic patch is 0.83° and the distance from the fixation square to the stimulus is 1.66°. The distance from the outer circle to the central test circle subtends 3.32°.

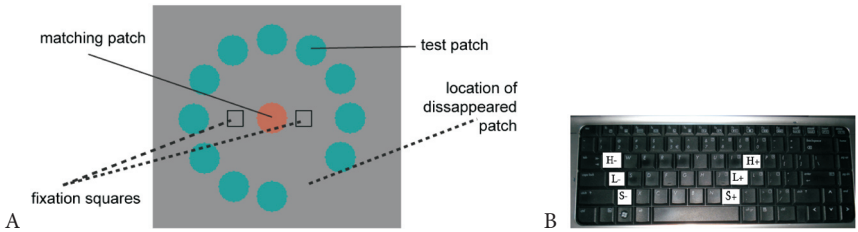

Fig. 4.1. **(Left) Experimental stimuli with 12 chromatic disks presented on the gray background. Color attributes of the test patch in the center are adjusted by experiment participant. (Right) Keyboard buttons associated with test patch color attributes in HSL color space.**

Presented 11 disks are of the same color, which is coded in the HSL color space and 30 hues are chosen for the experiment. Luminance values of the all 30 colors are matched to background luminance and measured with Konica Minolta CS-100A chroma meter.

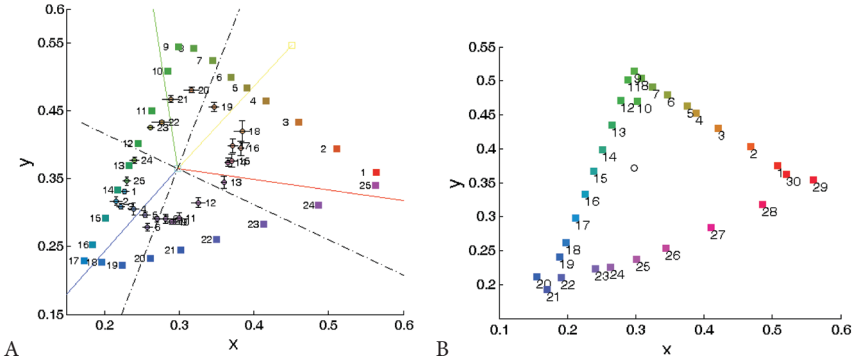

Fig. 4.2. **(A) Test colors (squares) and adjusted after-image complementary colors (circles) in CIE x,y chromaticity diagram. Black dashed lines represent the cardinal axes of the color space and colored solid lines show unique hue directions. Horizontal and vertical error bars showing standard errors for the average of five subjects. (B) Test stimuli colors defined for experiment in section 4.2.**

Stimuli colors used in our experiments are presented by squares in Fig. 4.2 (A). We have used HP Pavilion DV6555 PC with LCD monitor for purposes of this experiment. Figure 4.2 (B) shows color stimuli specified for experiment 4.2 for subjects with color vision anomalies. Differences in colors arise due to use of different monitors. Dell Inspiron 1525 with LCD monitor was used in experiments for anomalous color vision subjects. Portable computers were chosen to ease the procedure, because not always our subjects were able to participate in experiment visiting laboratory.

4.1.2. Results

First HSL color space arbitrary values were obtained, which later were transformed into RGB monitor digital values. Look-up table was applied to provide the chromaticity coordinates for CIE x,y diagram from RGB scalar values. The results show reliable data with correlation coeficient between the subjects of value 0,84± 0,03.

Adjusted complementary hues for five subjects are displayed in the CIE x, y chromaticity diagram (see Fig. 4.2). The saturation of complementary colors is lower compared to the test colors. Evaluated after-images usually produce offset from the plane relating test color with opposite color through the straight line. Least shifted after-images are the ones with the color No 19, 24, as well as No 6 and also No 13, which are the closest point of our test set to the cardinal directions of the physiological color space.

The 'triangular' arrangement of test colors produces four corners in the shape of the evaluated complementaries. The after-images of largest saturations placed in the corners of this shape are produced by stimuli No 2, 9, and 18 and also by stimuli No 20.

4.2. Complementary hues for color vision anomalous subjects

4.2.1. Subjects, stimuli and method

Three persons with color vision impairment took part in the complementary hue matching experiment (later abbreviated in form initial/age) - EL/22, JR/23, JE/62, as also one subject with normal color vision (21 years old) abbreviated as N. The selection of participants was carried out using the Ishihara color plates (Concise Ed., 1965) and Farnsworth D-15 test. Ishihara plate and Farnsworth D15 have diagnosed two of the participants (EL and JE) as protanomalous trichromats, while one participant (JR) as deuteranomalous trichromat. For less confusion we propose to indicate the subjects as follows:

ELp and JEp are identified as protanomalous trichromats; JRd – deuter-anomalous trichromat and N-normal trichromat.

To evaluate the after-image complementary colors for color anomalous subject we have used method described in the previous section 4.1.

4.2.2. Results

First, the CIE x, y coordinates of the obtained after-image colors were calculated. All of the anomalous subjects experienced difficulties in adjusting the after-images of the red and green test colors. From red to green test stimuli protanomalous subjects adjusted after-images of similar cyan colors of high saturation values similar to normal subject's adjusted saturation (but not hues). Deuteranomalous subject adjusted the after-images of lesser saturation for red to green (1^{st} till 12^{th}), but in the wider hues.

Anomalous participants experienced problems adjusting the after-images for cyanish test colors (13-16). Complementary hues were adjusted similar to the test cyan colors, either gray or highly shifted from the complementary, as opposite through the neutral point.

Test color lying close to the protanope confusion line (No 28) produces the after-image for anomalous persons similar to that of the normal trichromat. But test color on the deuteranope confusion line (No 27) showed a powerful decline from the normal trichromat adjusted.

In section 4.1 it was shown that complementary hues of after-images are produced in angles from the straight line drawn from the test color through the

neutral point. Matching of after-image colors by anomalous subjects produce severe declinations from the straight line. We have compared the shifts of the after-image complementaries for anomalous subjects with the shifts for normal subjects participated in this experiment (Fig. 4.3).

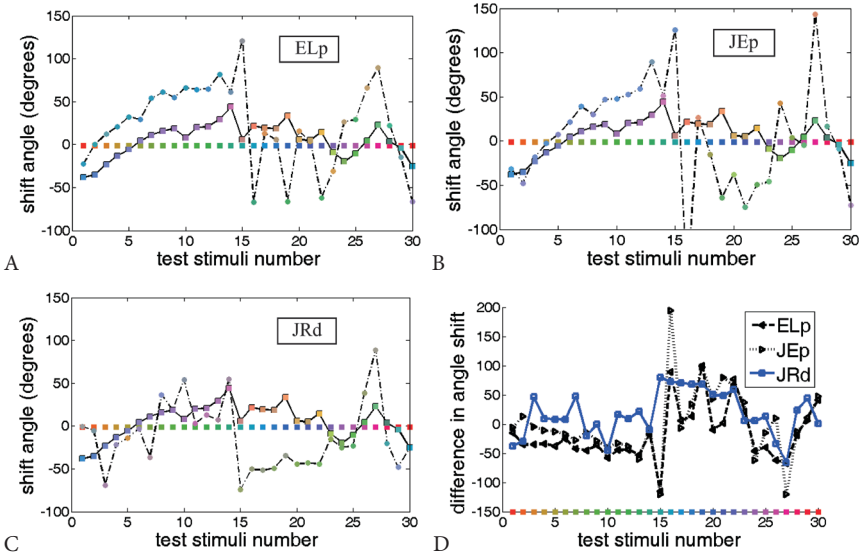

Fig. 4.3. **Shift of complementary hues of after-images in angle from the straight line going through the neutral point from the test color (from CIE x,y coordinates). Negative shifts represent induction to the counterclockwise direction from the straight line and positive values – clockwise direction. (A,B,C) solid lines with square markers show results for trichromat N, dashed lines and circle markers show shift for anomalous trichromats. (D) Angle difference between normal and anomalous subjects.**

The biggest angle shifts are seen for the protanomalous subjects adjusting after-images for green, cyan and blue test stimuli. The smallest shifts are observed for the red and yellow part of the spectrum. Obviously the largest shifts for all of the anomalous subjects are numbers: 15, 16 and 27.

Results for both of protanomalous subjects show similar trends with fewer variations for red, yellow and green test stimuli. Powerful fluctuations of after-images take part in the blue and violet stimuli. Deuteranomalous subject`s results are of different behavior with fluctuations present for red, yellow and green colors, there protanomalous show flat response. For cyan and blue stimuli

deuteranomalous subjects show no response fluctuations, comparing to the protanomalous.

Our results show interesting findings, which could be used for further investigation. However, no statistical data could be provided due to the limited number of subjects. In the present form experiment is time demanding, so number of test colors could be decreased substantially. We believe that further development of the method could lead to the wholesome technique in application for color vision diagnosis.

4. 3. Complementary hues of after-images in cardinal direction space

4.3.1. Stimuli, method and subjects

To study the after-images complementary hue mechanisms additional measurements were performed with stimuli, whose colors were chosen in the physiological color space (DKL). Squares in Fig. 4.4. (left) represent the test hues in DKL color space, where the x-axis is the LM cone signals and y-axis denotes the S and L + M cone mutual process. Test stimuli colors in DKL space were chosen on unity circle with axes normalized to 0.1 for x axis and 0.7 along the y axis to fit the monitor Gamut. Right graph of Fig. 4.4 shows stimuli colors in CIE x,y chromaticity diagram. Regardless of the elliptical shape of tests gamut, it is often used in color vision studies [43]. We tried to keep the saturation of colors as high as possible in relation to both DKL color space and CIE chromaticity diagram.

Six persons with normal color vision participated in the experiment, aged 20 to 28 years. Four of our subjects were males and two were of the female gender.

We have used the same experimental procedure as in experiments in section 4.1 and 4.2 with colors chosen in the DKL color space (Fig. 4.4 A). The subjects viewed the stimuli explained in section 4.1.1 and matched the perceived after-image in the central patch (see Fig. 4.1). Some preliminary measurements were done by subjects to understand the task of the experiment and procedure of color matching. Subjects made at least 10 measurements of the after-image complementary hue for each test stimuli.

4.3.2. Results

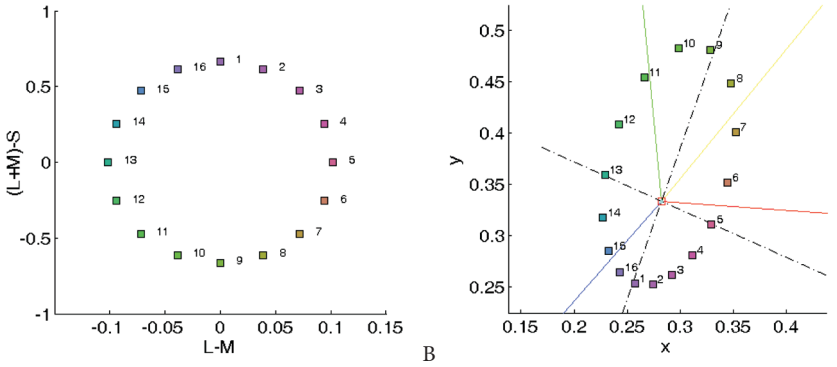

Fig. 4.4. **Stimuli colors in DKL color spaces (A) and in CIE x,y chromaticity diagram (B). Black dashed lines are cardinal directions of DKL color space.**

Fig. 4.5 shows the average values of the perceived after-image colors and their standard deviations indicated by error bars for five subjects. The bending of the after-image colors is similar to that observed in experiment in section 4.1. The graph on the right of Fig. 4.5 shows the luminance variations of matched after-images. Luminance set for background and stimuli is 25 cd/m^2. Matched after-images for the yellow and green stimuli (blue and violet) are a bit over the 25 cd/m^2 limit. Blue and red stimuli produce less luminous aftereffects. However, the variations of luminance are not significant.

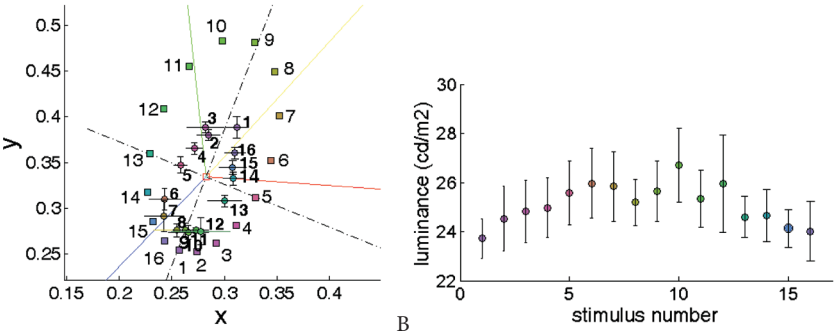

Fig. 4.5. **(A) Test stimuli colors (squares) and matched after-image colors (circles) in CIE x,y. Error bars indicate standard deviation. (B) Luminance variations of matched after-images. Test stimuli number on the x axis and evaluated luminance of the corresponding after-image on the y axis.**

The specific difference from experiment 4.1 is the ability to identify differential saturation of the aftereffect. The saturation values for each hue of the after-images can be analyzed in the DKL color space (Fig.4.6). The most saturated after-images are produced by the stimuli of yellow (No 6, 7, 8) and green (No 9, 10, 11, 12) hues, while pink and blues produces after-images of lower saturation. Color contrast for test stimuli and after-image is calculated in Fig. 4.6 (B). The most identical color contrast is perceived for after-images produced by stimuli No 5, 6, 7 and No 11, 12, 13. Saturation compression is observed for lime and green test colors, aligned on the lime-violet cardinal axis. Even greater compression is found for the blue and violet stimuli (No 1, 2, 15, 16) producing yellow and lime after-images.

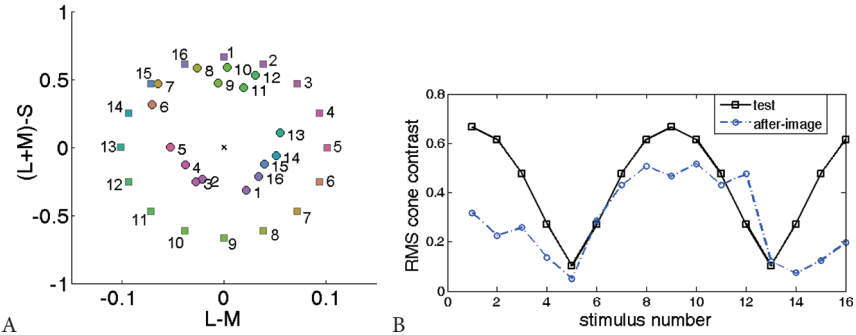

Fig. 4.6. **(A) Test colors (squares) and after-images (circles) in DKL color space. (B) Cone contrast for all test stimuli (squares, black line) produced after-images (circles, blue line).**

The obtained data is consistent with the results of our previous experiment, but provides valuable information on mechanisms of after-images. We have used trichromatic visual display to produce the after-images. The distributions of after-images in the CIE x,y diagram are similar to data from Wilson et al [24]. The shape of responses represented in DKL color space shows that yellow and green after-images produced by blue and violet stimuli are of lower saturations. Other after-images are similar in saturation values to that of the stimuli. Our findings are similar to the trends observed in color-contrast experiments with monochromatic sinusoidal gratings presented on the neutral background [44]. Similarly, to the results obtained by Switkes our results show greater saturations closer to 135 degrees then presented in DKL space.

4.4. Conclusions

1. Modification of “chaser” illusion is used to determine the hue, saturation and luminance of color after-images. Stimuli luminance was kept constant with the background and our preliminary study showed perfect correlation coefficients (0.84) between five experiment participants.
2. After-images defined for subjects with color vision anomaly, present significant deviations of after-images in the green-blue and violet colors (No 15, 16 and 27 with dominant wavelengths: 493nm, 487nm, and c. 502 nm). Found differences between after-images for normal and anomalous color vision can be developed as a color vision anomaly or deficiency alternative diagnostic method.
3. Saturation mechanisms for stimuli defined in DKL color space, show saturation value compression for yellow after-images, produced by blue stimuli. Our results resemble results obtained for the salience of chromatic contrast stimuli in chromoluminance space by E.Switkes [44].

5. EVALUATION OF AFTER-EFFECT FOR FILLING-IN BETWEEN THE CONTOURS

Four subjects (two males and two females, age from 27 to 30) with normal color vision participated in the study. Two of the participants are the authors of the research and two naïve subjects. Each of them underwent the experiment five times.

5.1. Experimental

Illusion based on the filling-in between the contours proposed by Van Lier *et al* [12] is used to produce the sensation of after-effect. The experimental approach is based on the judgment of the subjects about the strength of the perceived color after-effect between two chromatic pairs.

The colors of the stimuli were chosen based on the spectral irradiation of a computer display. To provide similar distances between the colors and differences in saturation, test colors were chosen in the CIE L*a*b* color space, with L value being equal to 60 units, and *a, b* values forming a circular shape with radius of 40 units. The lightness values chosen corresponded to luminance of 35 cd/m^2 (measured by Konica Minolta CS 100A chromameter). We chose a set of fifteen colors for our stimulus, which changed only in hue, keeping the brightness,

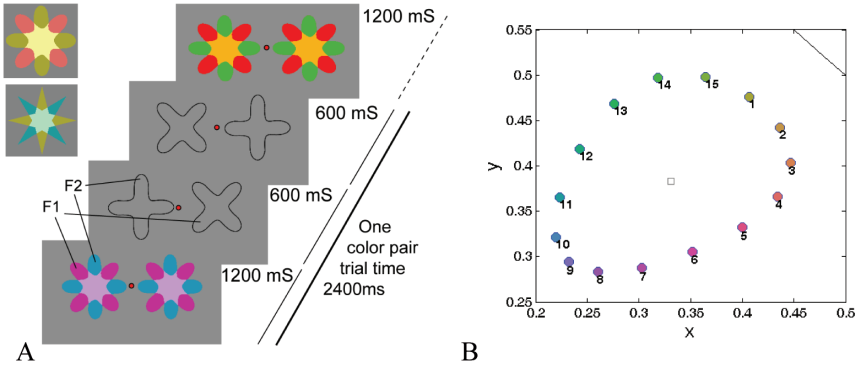

Fig. 5.1. **(A) Sequence setup of experimental stimuli. Colored shapes are presented for 1200 ms and replaced with empty shapes changing the directions by 45 degrees after 600ms. Contour orientation change produces switching of the after-effect colors from side to side. (B) Stimulus coordinates in CIE x,y chromaticity diagram truncated to the data.**

saturation and color differences constant. Fig. 5.1 shows the coordinates of test stimuli in the CIE *x, y* chromaticity diagram, with the number near the color spots indicating the coding of the sample.

A stimulus consists of four overlapping color Fig.s with two stimuli in each pair opposed to each other in 45 degrees (Fig. 5.1). Colors of the shapes overlap in additive way. Overlapped stimuli pairs are arranged on both sides of the fixation cross in 2.5 degrees of visual angle. The colors of all overlaping stimuli can be adjusted with the keyboard buttons. Both stimuli are presented for 1200 ms, after which black contours of the stimuli appear for 600ms, and, in the next 600 ms change their orientation by 45 degrees. As we have to change the colored figures in our stimuli, two variables representing the color of each Fig. were introduced: K1 for zero-rotated stimuli and K2 for diagonally rotated stimuli.

The subjects were instructed to make a judgment of the chromatic pair depending on the perceived strength of the after-effect. Before measurements, each of the participants underwent some trials to understand the purpose of the experiment and the after-effect evaluation procedure. The strength of a color pair was evaluated on the ten-grade scale by pressing button, from 1 to 0, (0 corresponds to 10 points). The lowest marks belong to the stimuli of the same colors.

5.2. Results

Average responses of all subjects where calculated for each pair of the stimuli. The responses could be represented in 15x15 cells matrix with ***x*** axis showing fixed colors and ***y*** axis for colors changed clockwise from the fixed color (Fig. 5.2). The lightness of the squares represents the strength judgment of perceived after-effect.

Surface plots in Fig. 5.2 obtained for two types of shapes differ in the distribution of the evaluation responses. For the round edge stimuli orange to green have the highest value and the second shape show strongest response pink to green. The responses cover quite a broad range and for some stimuli more than one peak can be observed. For example, tenth (blue) 'cross' stimuli produce effects with the sixth (yellow), eleventh (pink) position from itself. Similar examples can be found also for 'sharp edge' stimuli. A fifteenth (lime) stimulus is strong in cooperation with fifth (pink) and twelve (cyan) stimuli from it.

The most powerful responses have been obtained for the 1st color (yellow) paired with the 11th from it (cyanic blue), and for the 10th color (blue) paired with the 12th from it (pink), which is the 6th. The peak values for the round corner shape in Fig. 5.2 (left) produce continuous curve and follow rules similar to the complementary hues of after-images.

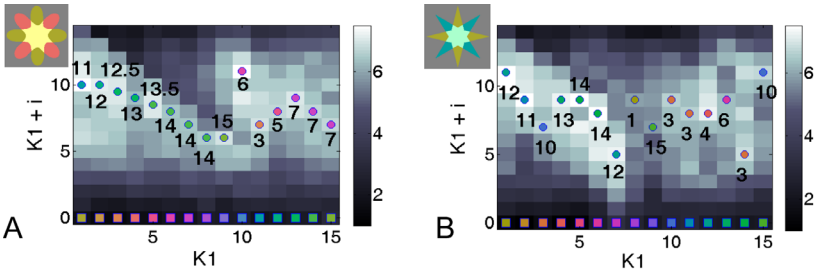

Fig. 5.2. **Surface representing strength of the filling-in for the pairs of K1 and K2. Average results of all subjects are depicted. The abscissa shows the first stimulus color (K1) and the ordinate – the sequence of the other fifteenth stimuli from K1, where i changes from 0 to 14. The squares in the lower part show K1 colors. The circles on the peaks of the surface represent number of K2 and a color sample.**

If we analyze the peaks of the obtained surface and plot the sample numbers (K2 in this case) on the peaks, two pronounced areas with K2 repetitions will be identified. These two areas belong to the colors green (K2 = 14) and pink (K2 = 7).

The results for each K1 for cover quite a broad range (except the peak value), and for some stimuli more than one peak can be observed. For example, the 10th (blue) stimulus is producing the sought-for effect with the 6th (lime, K2 = 15), the 10th (red, K2 = 4) and the 12th (pink, K2 = 6) positions from it. Also, interesting is the first color (yellow), which has two peaks with the 7th (violet, K2=7) and the 11th (cyan) from it.

Peak values in Figure 5.2 (right) for sharp corner shapes produce a spotty peak values, but we more peals for one stimulus (for example, K1= 5, 6, 11, 13, 14, and 15. To note, this stimuli correspond for red, pink, cyan and green colors.

To compare our findings with the theoretical lines of opponency and 'unique hues', the overall sum of the marks in all trials were calculated. There are color pairs which were judged low in most cases and also strong pairs judged with high marks. In such a way we tried to identify the colors most marked as strong in all trials. Fig. 5.3 shows the stimuli chromaticity coordinates in CIE x,y diagram. The size of the spot shows the occurrence of the particular color being rated with high value.

Comparing to our previous experiment on after-images particular experiment uses more complex stimuli and technique to evaluate the after-images. Filling-in is related to cortical processes and chosen experimental stimulus time (1200 ms) is insufficient to promote substantial retinal pigment bleaching [6].

Work of Capilla *et al* demonstrates the correspondence of physiological color spaces to color related processing stages in visual pathways from retina to cortex [46]. Opponent color mechanism space (DKL) [41, 45] corresponds to the level of the lateral geniculate nucleus color information processing level. On the other hand there is hue scaling studies which resulted in identification of 'unique' hues as a final color perception [43, 47]. However, determination of further chromatic information processing mechanisms behind LGN is difficult, due to differentiation of area V1 neurons chromatic sensitivity, as identified in electrophysiological studies [48]. A few years ago chromatic characteristics of glob cells were studied in area V4 [49]. Study suggested that this type of neurons is sensitive to the unique hues. Taking into account the neural nature of the filling-in phenomenon we have based our choice of stimulus similar to that of the receptive fields of V4 neurons.

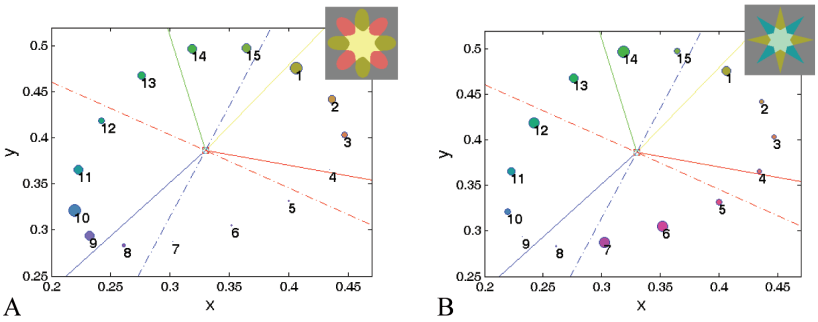

Fig. 5.3. **CIE xy, diagram with the occurrences of the most rated colors for two types of stimuli ((A) round edge, (B) sharp edge). Dashed lines represent cardinal directions of opponent color space [45]. Solid lines represent 'unique hue' directions [47].**

Similarly, to our previous experiments on after-images, we have found that stimuli of wider gamut produce after-effect with the same complementary color. The strongest weights identified in this manner belong to green (No 14) and magenta (No 7) for round edge stimuli. This allows for the conclusion that green and magenta colors play an important role in the formation of the after-effect. A fourteenth stimulus is roughly closest to the green unique hue and seventh is closest to the blue-yellow cardinal axis. Another interesting results is a tendency for some test stimuli (K1=1 or 10) to produce strong filling-in with colors which are not complementary, as identified in after-image matching experiments. It was found that the colors forming the most pronounced after-effects do not correspond to the 'unique hue' directions.

5.3. Conclusions

1. Pairs of chromatic stimuli with successive contour presentation were used to determine the strength of the perceived filling-in. Filling-in strength was evaluated for 225 color combinations for stimuli with round and sharp corners.
2. It was identified that shape of the object influence the evaluation of after-effect strength for filling-in. In contrast to expected results for the classic stimulus pairs (stimuli and its complementary) it was found that more than two color combinations from a dataset (for round corner shape if K1 = 1 then K2 is 7 and 11; K1 = 10 and K2= 4, 6, 12) can produce powerful filling-in.
3. For stimuli of round corners most pronounced after-images coincide with least changing axis from after-image complementary hue matching experiments (sections 4.1, 4.3), indicating stimuli No 7 and No 14 are important color axes in formation of after-images.

THESIS

1. Orthogonally oriented context in texture segregation task have shown no significant altering of the perception threshold. Presence of collinear context reduces the detection threshold on average by 26%.
2. Subthreshold stimulation to better-seeing eye (from 1.25 to 10 ms) in case of amblyopia significantly improves the detection threshold in amblyopic eye (at 5 and 7.5 ms stimulation, similar to the better-seeing eye results). Results show improvements of reaction times.
3. Multispectral imaging allowed simulating the performance of pseudoisochromatic plate under daylight and fluorescent lighting. Applying provided analysis it was identified that Ishihara plate (No 13) performs better in daylight conditions that the Rabkin test (No 17) in daylight conditions. The analytical method includes impact of lighting and provides possibility to designate cone signals, and is a suitable tool for the exploration of existing and development of novel pseudoisochromatic plates.
4. Measurements of the after-images hues for anomalous trichromats deviations of complementary colors are identified in blue and green-violet spectrum (dominant wavelengths: 495nm, 487nm, and c.502 nm). Found differences between hues of after-images can be developed as diagnostic method for color vision impairment.
5. In filling-in between the contours it was shown, that strong after-effects are obtained not only for the classic stimulus pairs (test and complementary), but also for other color combinations (with K1 = 1 K2 = 7, 11, K1 = K2 = 10 with 4, 6, 12). Different strength for after-images was identified for round and sharp corner shapes. After-images for round corner stimuli coincide with the experimental results on complementary hues of after-images, indicating two pronounced color axes (stimulus No 7 and No 14).

SUMMARY AND PROPOSED APPLICATIONS

Perceptual training with temporary textured objects significantly improves the detection threshold and show reaction time improvements. The largest effect is obtained for stimuli red-green stimuli of lowest luminance contrast. Contextual modulation experiments for experienced subjects showed collinear oriented peripheral stimulus suppressive effect on the central stimulus perception threshold. To improve the perceptual characteristics in amblyopia, method uses ferroelectric glasses to ensure the sub-threshold stimulation to the better-seeing eye and a brief stimulus recognition task with amblyopic eye. The results show recognition threshold improvement in amblyopic eye. The proposed method is applicable for perceptual training in amblyopia and further clinical research.

The proposed pseudoisochromatic plate analysis uses machine vision object recognition algorithm is ready to be used for evaluation of performance of existing tests and can be a valuable tool when creating new tests. The method comprises the lighting effects on the diagnostic abilities of the test and allows creating tests suitable for different lighting conditions. The latent object perception is dependent on the color information; method behaves as a simple impaired color vision simulation algorithm. Another benefit could be provided by possibility to apply the models of color constancy and color induction.

Differences were found in complementary hues of after-images for subjects with normal and anomalous color vision. Probably, dichromate subjects would present even more pronounced differences. To be acceptable for clinical applications for color vision screening, it is necessary to reduce the number of test colors, which should result in least trial time. Regardless of our findings, more thorough clinical investigation would be necessary about the errors, before method could be acceptable for diagnostic purposes.

It was found that filling-in between contours produce different strength after-effect for round and sharp corner shapes. In case of round corner stimuli two salient axes are similar to that found for complementary hues of after-images.

PUBLICATIONS

1. Zarina, L., Fomins, S. (2010). Collinear suppression in texture segmentation for temporally modulated stimuli. *Latvian Journal of Physics and Technical Science*, Vol. 47(3), 31–36.
2. Fomins, S., Ozolinsh, M., Krumina, G., Karitans, V. (2008). Ferroelectric liquid crystal glasses for amblyopia research. *Integrated Ferroelectrics*, 103, pp. 10–17.
3. Ozolinsh, M., Fomins, S. (2010). Multispectral color analysis for quantitative evaluation of pseudoisochromatic color deficiency tests. *Proc. SPIE*, Vol. 7845, 78450J; doi:10.1117/12.871846.
4. Fomins, S., Rileyeva-Piskura, N. (2010). Strength judgment of filling-in color illusion. *Latvian Journal of Physics and Technical Science*, Vol. 47(3), 44–50.
5. Fomins, S., Ozolinsh, M. (2010). Multispectral Analysis of Color Vision Deficiency Tests. *Materials Science (Medžiagotyra). (in press)*
6. Ozolinsh, M., Andersson, G., Krumina, G., Fomins, S. (2008). Spectral and temporal characteristics of liquid crystal goggles for vision research. *Integrated Ferroelectrics*, Volume 103, pp. 1–9.
7. Fomins, S., Reinfelde, M., Larichev, A., Iroshnikov, N., Gerbreders, A., Ozolinsh, M. (2008). Photoinduced AsSeS thin film phase plates as adaptive optics mirrors for eye aberration correction. *SPIE, Vol. 7142*, 71421C.
8. Ozolinsh, M., Colomb, M., Lauva, D., Fomins, S. and Morange, P. (2010) Mesopic vision characteristics at decreased contrast in fog. *Proc. SPIE*, Vol. 7853, 785342; doi:10.1117/12.871838.
9. Ozolinsh, M., Fomins, S., Colomb, M. (2004) „Optotypes for human color contrast sensitivity tests". *Proc. OSAV'2004*, *Optical Sensing and Artificial Vision*, ITMO, Saint Petersburg, Russia, pp. 351–356.
10. Ozolinsh, M., Ikaunieks, G., and Fomins, S. (2005) Color Vision Experimental Studies in Teaching of Optometry. *Proc. „Education and Training in Optics and Photonics." Pole Optique et Photonique,* Marseille, pp. 295–297.

CONFERENCE ABSTRACTS

1. **29th European Conference on Visual Perception**, Saint Petersburg, Russia, August 20–26, 2006. **Fomins, S., Ozolinsh, M., and Parkkinen, J.** „Search experiments with the blurred color stimuli", *Perception. ECVP Abstract Supplement*, 35, p. 87.
2. **30th European Conference on Visual Perception**, Arezzo, Italy, August 27–31, 2007. **Fomins, S, Ozolinsh, M., Ikaunieks, G**. "Temporal stimuli and texture segmentation." *Perception. ECVP Abstract Supplement,* 36, p. 44.
3. **30th European Conference on Visual Perception**, Arezzo, Italy, August 27–31, 2007. **Ikaunieks, G., Ozolinsh, M., Fomins, S.** Light-scattering effect on color-pattern VEP response. *Perception. ECVP Abstract Supplement,* 36, p. 39.
4. **31th European Conference on Visual Perception**, Utrecht, Netherlands, August 24–28, 2008. **Fomins, S**. "Masking study of instant stimuli texture segmentation" *Perception. ECVP Abstract Supplement* 37, p. 80.
5. **32th European Conference on Visual Perception**, Regensburg, Germany, Aug 24–28, 2009. **Ozolinsh, M., Colomb, M., Ikaunieks, G., Fomins, S., Morange, P.** Visual acuity at low illuminance and contrast in fog. *Perception. ECVP Abstract Supplement*, 38, p. 45.
6. **32th European Conference on Visual Perception**, Regensburg, Germany, Aug 24–28, 2009. **Fomins, S., Zariņa, L.** Segmentation of instant isoluminant chromatic textures. *Perception. ECVP Abstract Supplement,* 38, p. 54.
7. **32th European Conference on Visual Perception**, Regensburg, Germany, August 24–28, 2009. **Atvars, U., Fomins, S**. Chaser illusion and opponent color aftereffects. *Perception. ECVP Abstract Supplement,* 38, p.135.
8. **32th European Conference on Visual Perception**, Regensburg, Germany, August 24–28, 2009. **Ozolinsh, M., Fomins, S**. Multispectral analysis of the color deficiency tests and modelling of cones influence on test perception. *Perception. ECVP Abstract Supplement,* 38, p. 37.
9. **32th European Conference on Visual Perception**, Regensburg, Germany, August 24–28, 2009. **Lauva, D., Ozolinsh, M., Fomins, S.** Modelling of RGB color contribution to visual acuity in conditions of fog evoked decrease of luminance and contrast. *Perception. ECVP Abstract Supplement,* 38, p. 35.
10. **33th European Conference on Visual Perception**, Lausanne, Switzerland, August 22–26, 2010. **Fomins, S., Rileyeva-Piskura, N**. Strength judgment of filling-in color aftereffect illusion for different shapes. *Perception. ECVP Abstract Supplement*, 39, p. 86.

11. **Functional materials and nanotechnologies (FMNT`07)**, Riga, Latvia, April 2–4, 2007. **Ozolinsh, M., Fomins, S., Ikaunieks, G.** "Eye aberration dynamics studies using Hartman-Shack aberrometer," *Book of Abstracts*, p. 137.
12. **Functional materials and nanotechnologies (FMNT`08)**, Riga, Latvia, April 1–4, *2008.* **Fomins, S., Ozolinsh, M., Krumina, G., Karitans, V**. Ferroelectric Liquid Crystal Glasses for Amblyopia Training. *Book of Abstracts*, p. 132.
13. **Functional materials and nanotechnologies (FMNT'09)**, Riga, Latvia, March 31–April 3, 2009. **Fomins, S., Ozolinsh, M.** Multispectral analysis of color deficiency tests and modelling of cone influence on perception of color. *Book of Abstracts,* p. 203.
14. **20th symposium of International Color Vision Society (ICVS'09)**, Portugal, Braga, 24–28 July, 2009**. Martín, I., Fomins, S., Ozolinsh, M.** Multispectral analysis of color deficiency tests and modelling of cones influence on test perception. *Abstract Booklet*, p. 145.
15. **Annual Meeting of Applied Vision Association – *2006 "Vision in Perception and Cognition".*** Bradford University, England, April 4, 2006. **Ozolinsh, M., Ikaunieks, G., Fomins, S., Colomb, M., Parkkinen, J.** Perception of Color Contrast Stimuli in the Presence of Scattering. *Abstracts*, p. 5.
16. **Annual Meeting of European Optical Society**, Paris, France, October, 2006**. Ozolinsh, M., Ikaunieks G., and Fomins, S**. Dynamics of Eye Aberration Detected by High-Speed Hartmann-Shack Aberrometer. *Proceedings*, pp. 92–93.
17. **The 13th AVA Christmas Meeting,** Bristol, December 19, 2008. **Ozolinsh, M., Colomb, M., Ikaunieks, G., Fomins, S. and Morange, P.** Visual acuity at low illuminance and contrast in fog. *AVA meeting abstracts*. p. 25.
18. **AVA 14th Christmas Meeting 2009,** University of Bristol, December 18, 2009. **Ozolinsh, M., Fomins, S., Colomb, M.** Quantitative evaluation of Ishihara and Rabkin color deficiency tests using multispectral color analysis. *AVA meeting abstracts*, p. 29.
19. **Advanced Optical Materials and Devices (AOMD-06)**, Riga, Latvia, August 24–27, 2008. **Fomins, S., Ozolinsh, M., Krumina, G., Karitans, V.** Ferroelectric liquid crystal glasses for vision research. *Programme and Abstracts,* p. 88.
20. **Advanced Optical Materials and Devices (AOMD-06)**, Riga, Latvia, August 24–27, 2008. **Sarakovskis, A., Grube, J., Dimitrocenko, L., Fomins, S., Springis, M.** Up-conversion luminescence studies on Er^{3+}, Yb^{3+} and Tm^{3+}

doped oxyfluoride glass and glass ceramics. *Programme and Abstracts*, p. 51.

21. **Development in Optics and Comunications (DOC'06)**, Riga, April 28–30, 2006. **Fomins, S., Karitans, V., Ikaunieks, G., Ozolinsh, M.** Saliency based visual attention and the visual search task. *DOC`06 Abstracts,* p. 30–32.
22. **Development in Optics and Communications (DOC'08)**, Riga, April 28–30, 2008. **Fomins, S.** Masking study of instant stimuli texture segmentation. *Abstracts*, p. 5.
23. **Development in Optics and Communications (DOC'09)**, Riga, April 24–26, 2009. **Fomins, S., Ozolinsh, M., Atvars, U.** Multispectral analysis of the color deficiency tests and modelling of interpretation by trichromat color systems. *Abstracts*, p.43–44.
24. **Development in Optics and Communications (DOC'09)**, Riga, April 24–26, 2009. **Atvars, U., Fomins, S.** Chaser illusion and opponent color after-effects. *Abstracts*, p. 45.
25. **Development in Optics and Communications (DOC`10)**, Riga, April 23–25, 2010. **Fomins, S., Rileyeva-Piskura, N**. Chromatic aftereffect strength for different shapes. *Abstracts*, p. 29.
26. **Development in Optics and Communications (DOC`10)**, Riga, April 23–25, 2010. **Zarina, L., Fomins, S.** Collinear suppression in texture segmentation for temporally modulated stimuli. *Abstracts*, p.32.
27. **The 12th International School-Conference "ADVANCED MATERIALS AND TECHNOLOGIES"**, Palanga, Lietuva, August 27–31, 2010. **Fomins, S., Ozolinsh, M**. Multispectral analysis of color deficiency tests and modeling of cones influence on perception of color. *Book of Abstracts*, p. 38.
28. **SPIE/COS Photonics Asia**, Beijing, China, October 18–20**,** 2010. **Ozolinsh, M., Fomins, S.** Multispectral color analysis for quantitative evaluation of pseudoisochromatic color deficiency tests. *Abstract Summaries*, p. 33.

LITERATURE

1. Polat, U., Mizobe, K., Pettet, M.W., Kasamatsu, T., Norcia, A.M. (1998). Collinear stimuli regulate visual responses depending on cell's contrast threshold. *Nature* 391, 580–584.
2. Li, Z. (1999). Primary visual cortex as a saliency network for pre-attentive segmentation. *In: 3rd Annual Vision Research Conference Pre-attentive and Attentive Mechanisms in Vision*, Florida, USA, May 7–8
3. Tucker, T.R., Fitzpatrick, D. (2004). Contribution of vertical and horizontal circuits to the response properties of neurons in primary visual cortex. Chalupa, L. M., Werner, J. S. *The visual neurosciences*. Vol. 2. Cambridge, Massachusetts, London, England: A Bradford Book The MIT Press
4. Cass, J.R., Spehar, B. (2006). Dynamics of collinear contrast facilitation are consistent with long-range horizontal striate transmission. Vis Res 45, 2728–2739.
5. Wright, W.K. (1955). Pediatric ophthalmology and strabismus, Mosby, pp.45–57
6. Rushton, W.A.H., Henry, G.H. (1968). Bleaching and regeneration of cone pigments in man. *Vis Res* 8(6), Pages 617–631
7. Loomis, J. M. (1972). The photopigment bleaching hypothesis of complementary afterimages: A psychophysical test, *Vis Res* 12, 1587–1594.
8. Shevell, S.K., St Clair, R., Hong, S.W. (2008). Misbinding of color to form in afterimages. *Vis Neurosci* 25(3):355–60.
9. Komatsu, H. (2006). The neural mechanisms of perceptual filling-in. *Nature Reviews Neuroscience* 7, 220–231. Doi: 10.1038/nrn1869.
10. Brettel, H., Viénot, F., Mollon, J.D. (1997). Computerized simulation of color appearance for dichromats. *J. Opt. Soc. Am*. A 14, 2647–2655.
11. Capilla, P., Díez-Ajenjo, M.A., Luque, M.J., Malo, J. (2004).Corresponding-pair procedure: a new approach to simulation of dichromatic color perception. *J. Opt. Soc. Am*. A 21, 176–186
12. Van Lier, R., Vergeer, M., Anstis, S. (2009). Filling-in afterimage colors between the lines. *Current Biology*, 19(8), R323–R324.
13. Felleman, D.J., Van Essen, D.C. (1991). Distributed hierarchical processing in primate cerebral cortex. **Cerebral Cortex** 1, 1–47.
14. Underleider, L.G., Mishkin, M. (1982). Two cortical visual systems. In *Analysis of Visual Behavior*. Ingle, D.J., Goodale, M.A., Masfield, R.J.W. MIT Press, Cambridge, 549–586.
15. Heinrich, S.P., Andrés, M., Bach, M. (2007). Attention and visual texture segregation, *Journal of vision*, Vol.7 (6), 1–10.
16. Palmer, S.E. (1999). *Vision science, Photons to phenomenology*. London, A Bradford Book, The MIT Press.

17. Kashi, R., Papathomas, T.V., Julesz, B. (2002). Psychophysics and modelling of texture segregation. Models of the visual system. G.K.Hung, K.J.Cuiffreda. Kluwer academic, New York. pp.465–486.
18. Breitmeyer, B.G., Ogmen, H. (2007). Visual masking, *Scholarpedia* – Vol.2 (7), 3330.
19. Francis, G. (1997). Cortical Dynamics of Lateral Inhibition: Metacontrast Masking. *Psychologycal Review,* 104 (3), 572–594.
20. Shimojo, S., Kamitani, Y., Nishida, S. (2001). Aterimage of Perceptually Filled-in Surface. *Science* 293, 1677–1680.
21. Schwarz, S. H. (2004). *Visual Perception: A Clinical Orientation. Third Edition.* United States of America: The McGraw-Hill, p.471.
22. Birch, J. (2001). Diagnosis of defective color vision. Second edition, Butterworth-Heinemann, Edinburg.
23. Smith, V. C., Pokorny, J. (1975). Spectral Sensitivity of the Foveal Cone Photopigments between 400 and 500 nm. *Vis Res,* 15, 161 – 171.
24. Wilson, M. H., Brocklebank, R. W. (1955). Complementary Hues of After-Images. *J. Opt. Soc. Am*. 45, 293–299.
25. Scialfa, C.T., Hamaluk E. (2001). Aging, Texture Segmentation, and Exposure Duration: Evidence for a Deficit Is Preattentive Processing. *Experimental Aging Research* 27, 123–135
26. Cuifredda, K.J., Levi, D.M., Selenow, A. (1991). Amblyopia: Basic and clinical aspects. Boston: Butterworth-Heinemann.
27. BenEzra, O., Herzog, R., Cohen, E., Karshai, I., BenEzra, D. (2007). Liquid crystal glasses: feasibility and safety of a new modality for treating amblyopia. *Arch Ophthalm*, 125 (4), 580–1.
28. Vedamurthy, I., Suttle, C.M., Alexander, J., Asper, L.J. (2007). Interocular interactions during acuity measurement in children and adults, and in adults with amblyopia. *Vis Res*, 47, 179–188.
29. http://www.displaytech.com/photonics_shutters.html. Displaytech photonic shutters. (Retrieved on April 2, 2008).
30. Barett, B.T., Bradley, A., McGraw, P.V. (2004). Understanding the basis of amblyopia. *Neuroscientist* 10(2), 106–17.
31. Kiorpes, L., Kiper, D.C., O'Keefe, L.P., Cavanaugh, J.R., Movshon, J.A. (1998). Neuronal Correlates of Amblyopia in the Visual Cortex of Macaque Monkeys with Experimental Strabismus and Anisometropia. *The Journal of Neuroscience* 18(16), 6411–6424.
32. Moschos, M.M., Margetis, I., Tsapakis, S., Panagakis, G., Chatzistephanou, I.K., Iliakis, E. (2010). Multifocal visual evoked potentials in amblyopia due to anisometropia. *Clinical Ophthalmology* 4, 849–853.
33. *Рабкин, Е. Б. (*1998*). Полихроматические таблицы для исследования цветоощущения*. (10th ed.). Ю.Сапожков, Minsk.

[Rabkin, E.B. (1998). Polychromatic plates for color perception examination. 10th Edition, *Sapozhkov, Y.*, Minsk].

34. Ishihara, S. (1965). Ishihara`s test for color blindness. Concise Edition, Isshinkai, Tokyo, Japan.
35. Stockman, A., Sharpe, L. T. (2000). Spectral sensitivities of the middle- and long-wavelength sensitive cones derived from measurements in observers of known genotype. *Vision Res* 40, 1711–1737.
36. Mancuso, K., Mauck, M.C., Kuchenbecker, J.A., Neitz, M., & Neitz, J. (2010). A multi-stage color model revisited: Implications for a gene therapy cure for red-green colorblindness. In R.E. Anderson, J.G. Hollyfield, & M.M. LaVail (Eds.), Advances in Experimental Medicine and Biology. New York, USA: Springer New York. 631–638.
37. Cole, B.L., Lian, K. Y., Lakkis, G. (2006). The ne Richmond HRR pseudoisochromatic test for color vision is better than the Ishihara test. *Clin Exp Optometry* 89(2), 73–80.
38. Dain, S.J., Gray, S., Tran, L. (1998). Colorimetric analysis and performance assessment of the Hahn new pseudoisochromatic color vision test. *Color research and application. Supplement* 23(2), 69–77.
39. Bailey, J.E., Neitz, M., Tait, D. M., Neitz, J. (2004). Evaluation of an updated HRR color vision test. *Vis Neuroscience* 21, 431–436.
40. Johnson, G.M., Fairchild, M.D. (2003). Visual psychophysics and color appearance. *CRC Digital Color Imaging Handbook*, 115–171.
41. Stockman, A., Brainard, H.D. (2010). Color vision mechanisms. In the OSA Handbook of Optics (3rd edition, M. Bass, ed). McGraw-Hill, New York, 11.1–11.104.
42. Blue, R.C. 2005. A visual yet non-optical subjective intonation. *Electroneurobiología* 13 (3), 299–300.
43. De Valois, R.L., De Valois, K.K., Switkes, E., Mahon, L. (1997). Hue Scaling of Isoluminant and Cone-specific Lights. *Vis Res* 37(7), 885–897.
44. Switkes, E. (2008). Contrast salience across three-dimensional chromoluminance space. *Vis Res* 48, 1812–1819.
45. Derrington, A.M., Krauskopf, J., Lennie, P. (1984). Chromatic mechanisms in lateral geniculate nucleus of macaque. *J. Physiol.* 357, 241–265.
46. Capilla, P., Malo, J., Luque, M.J., Artigas, J.M. (1998). Color representation spaces at different physiological levels: a comparative analysis. *Journal of Optics* 29, 324–338.
47. Miyahara, E. (2003). Focal colors and unique hues. *Percept Mot Skills* 97(3): 1038–1042.
48. Gegenfurtner, K.R. (2003). Cortical mechanisms of color vision. *Nature Reviews Neuroscience* 4, 563–572.
49. Stoughton, C.M., Conway, B.V. (2008). Neural basis for unique hues. *Current Biology 18* (16), R698–R699.

ACKNOWLEDGEMENT

I would like to express my gratitude to European Social Fund, Latvian National Research program for financial support. Many thanks to supervisor professor Māris Ozoliņš for proposed ideas and provided solutions for their implementation. I am grateful to friends and colleagues at the Optometry and Vision Science Department, as also to colleagues at Institute of Solid State Physics.

Zelta Rudens
tipogrāfija